Customizing the Following Behavior Models to Mimic the Weak lane based Mixed Traffic Conditions

Raju, Narayana; Arkatkar, Shriniwas; Easa, Said; Joshi, Gaurang

Important note
To cite this publication, please use the final published version (if applicable).
Please check the document version above.

Customizing the following behavior models to mimic the weak lane based mixed traffic conditions

Narayana Raju, Shriniwas Arkatkar, Said Easa & Gaurang Joshi

Published online: 29 Jul 2021.

Submit your article to this journal

View related articles

View Crossmark data

Taylor & Francis
Taylor & Francis Group

Check for updates

Customizing the following behavior models to mimic the weak lane based mixed traffic conditions

Narayana Raju [a,b], Shriniwas Arkatkar [b], Said Easa [c] and Gaurang Joshi [b]

[a]Transportation and Planning, Delft University of Technology, Stevinweg 1, 2628 CN Delft, The Netherlands; [b]Civil Engineering Department, Sardar Vallabhbhai National Institute of Technology, Surat, India; [c]Civil Engineering Department, Ryerson University, Toronto, Canada

ABSTRACT

This study aims to model traffic flow under weak lane based heterogonous (mixed) traffic conditions. Unlike homogeneous traffic, when a follower (subject) vehicle in mixed traffic moves closer to its leader vehicle, it tends to adjust its longitudinal movement or change its lane and acts discretely. Due to this phenomenon, traffic flow modeling under such conditions is always challenging. A new driver behavioral logic is conceptualized for the vehicles' movement within a combination of surrounding vehicles. In which the following behavior was dissected with the lateral shift distance between vehicles. Two car-following models for homogeneous traffic conditions, the IDM and Gipps models were adapted with relevant lateral behavior parameters to different vehicle classes under mixed-traffic conditions. The new driving behavior logic was incorporated externally in place of default logic. The results showed that the performance of the adapted models was better accurate than the classical models.

Introduction

The car-following model is one of the most relevant notions in modeling the following behavior among the vehicles. Simultaneously, with the stochastic nature of driving behavior, the following behavior is a complex phenomenon in traffic science. To understand this, researchers developed several car-following models to mimic traffic behavior in the past. Pipes (1953) related the follower's speed (subject) vehicle to the gap with the leader vehicle and modeled the following behavior, an initial attempt in traffic-flow modeling. Researchers formulated different car-following models to replicate the following behavior and model the traffic flow (Forbes et al. 1959; Gazis, Herman, and Rothery 1961; Gazis, Herman, and Potts 1959). To a certain extent, these models replicated the following behavior on an aggregate level. The substantial human involvement in driving following behavior logics has led to the concept of various car-following models for replicating traffic dynamics; particularly at the micro level (Wiedemann 1974; Newell 1961; van Winsum 1999; Laws 1981; Tang et al. 2017; Gipps 1981; Treiber, Hennecke, and Helbing 2000).

Given the microscopic nature, understanding the following behavior among the vehicles demands time–space data of the vehicles. With the data constraints, the performance of car-following models was initially limited to specific traffic scenarios. Considering the importance of the following behavior, numerous studies (Johansson and Rumar 1971; Toledo, Koutsopoulos, and Ben-Akiva 2003; Wang et al. 2015) are attempted and integrated with traffic flow modeling for better insights. The main objective

---

CONTACT Shriniwas Arkatkar ✉ sarkatkar@gmail.com

is to devise/develop the following models which may be confirmed realistically to the field conditions. With the advent and availability of computing techniques, numerous following behavior studies are performed over time, for example, which includes human elements (van Winsum 1999), the impact of road infrastructure (Oviedo-Trespalacios et al. 2017), drivers perspective (Boer 1999), the impact of road tunnels in following behavior (Yeung and Wong 2014). Simultaneously, researchers also revealed the importance of studying the vehicles' lateral movement behavior (Zheng 2014; Toledo, Koutsopoulos, and Ben-Akiva 2009; Hidas 2002; Keyvan-Ekbatani, Knoop, and Daamen 2016; Li et al. 2016). This has also led to modeling different lane-change driving behavior, particularly under homogeneous and lane-based traffic conditions in developed countries.

With advancements in technology, microscopic traffic simulation plays a considerable role in traffic flow modeling. The simulation tools assembled with different behavioral rationalities, such as car-following models (mostly psycho-physical models), lane-change logics, and gap-acceptance models, as a combined package. This provides a considerable opportunity for modeling driving behavior using simulation experiments and offers countless chances of mimicking real-field conditions reasonably well. Numerous studies were reported, including evaluation of freeway control (Ben-Akiva et al. 2003; Ngoduy 2012), emissions (Jie et al. 2013; Guzman and Orjuela 2017; Zhu, Lo, and Lin 2013), ramp control (Antonov and Kurlov 2002; Xu et al. 2019), pedestrian flow (Løvås 1994; Lee et al. 2018), and safety assessment (Lima Azevedo et al. 2015). With other numerous outcomes, traffic flow studies are also taken up to the next level based on microsimulation tools. Simultaneously, it has resulted in high customization options in simulation models and diversely rich plenteous microscopic field inputs to provide well-calibrated models in the simulation process. However, capturing such microscopic interactions among vehicles from real-field conditions advocates the development of a high-quality vehicular trajectory database that may better capture the traffic stream's driver responses reasonably well.

Thus, studying the following behavior warrants high-quality trajectory data, where the vehicular positions from the traffic must be tracked with the smallest possible update interval. Assessing this research gap, the United States (US) Federal Highway Administration (FHWA), as a part of the NGSIM project, developed a vehicular trajectory dataset using automated image processing tools at different locations for a trap length of 400–600 m for different classes of roadway facilities (FHWA 2007). NGSIM dataset acts as one of the prime sources in understating the following behavior under lane-based homogeneous traffic conditions prevailing in the US. On these lines, numerous studies were performed, oscillations in following behavior (D. Chen et al. 2012), latent class functions (Koutsopoulos and Farah 2012), deep learning (Zhang et al. 2019), modeling autonomous following behavior (Rahmati et al. 2019).

In the present work, to refer weak lane-discipline heterogeneous traffic conditions, the authors adopted the term 'mixed traffic.' At the same time, the authors are not referring to the mixed traffic of autonomous and human-driven vehicles. To understand the driving behavior in mixed traffic conditions, research attempts (Venkatesan, Gowri, and Sivanandan 2008; Mallikarjuna and Rao 2011) were carried in recent times. In this direction, Kanagaraj et al. (2015) highlighted the importance of lateral behavior in mixed traffic conditions. On similar lines, studies (Das et al. 2020; Raju et al. 2018) highlighted the smaller vehicle's lateral maneuverability in impacting the traffic stream conditions. Further, researchers (Paul et al. 2021) inferred that segregating smaller vehicles in mixed traffic streams can improve road networks' safety and efficiency. On similar lines, few other studies reported substantial lateral behavior of vehicles and smaller vehicles' dominance in the traffic stream (Bharadwaj et al. 2016; Raju et al. 2018). In this domain (Sharath and Velaga 2020; Raju, Arkatkar, and Gaurang 2019), highlighted the importance of surrounding vehicles' can impact the vehicle's movement in a mixed traffic stream. Further, a study by Patil et al. (2021) explicitly highlights the importance of surrounding vehicles in surrogate traffic safety. Simultaneously, researchers attempted to calibrate the established car-following and lane-change models of homogeneous traffic for mixed-traffic data, including (Raju, Arkatkar, and Joshi 2020; Raju, Arkatkar, and Gaurang 2019).
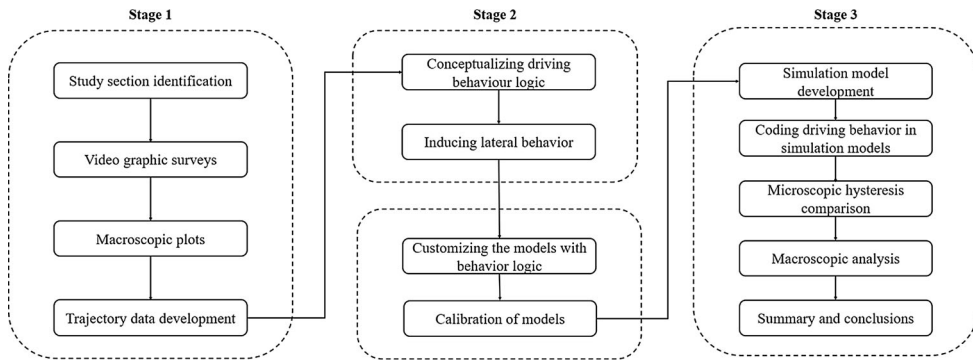
**Figure 1.** The methodological framework adopted in the study.

In the case of mixed-traffic conditions prevailing in India, different vehicle categories exist on the roads. This is also coupled with ensuing weak lane discipline that results in complex interactions among the vehicles. This may be attributed to many possible combinations of longitudinal and lateral gaps as a function of the static and dynamic characteristics. Under these conditions, even the well-established car-following models tend to underperform. As a result, the benefits of traffic flow modeling concepts tend to remain underutilized, and studies have not succeeded in inducing the real, naturalistic sense of mixed-traffic movement. Thus, modeling of mixed-traffic conditions forms a clear research gap. Given the research gaps pronounced from the literature review, it is realized that the study of driving behavior under homogeneous and mixed-traffic conditions is a must for modeling traffic flow precisely. Accordingly, the research work is devised in three stages, as shown in Figure 1. The initial stage is about the identification of the study section, followed by trajectory data development. In the second stage, driving behavior logic is conceptualized, and the selected driving behavior models are customized with the lateral movement of the vehicles in the surrounding of the subject vehicle. Based on the field trajectory data, the customized driving behavior models are well-calibrated. In the final stage of the work, to model the mixed traffic conditions, the calibrated driving behavior models are coded in the micro-simulation tool PTV VISSIM, 11.0. Further, the models' performance is evaluated both at microscopic hysteresis as well as macroscopic levels, and the detailed results are presented, demonstrating the complexity involved in capturing longitudinal and lateral driving behaviors simultaneously under mixed-traffic conditions.

Study Section

An experiment was designed to address the challenges in traffic flow modeling under mixed-traffic conditions, considering diverse roadway and traffic conditions. A segment on the western expressway in India was considered for this purpose. A wide variation in traffic flow existed, ranging from free-flow to near-capacity flow, and stop-and-go conditions in the congested regime. Video graphic surveys were conducted, and macroscopic plots were developed. Further, high-quality trajectory data were developed at three different flow levels for this section to sense driving behavior. In considering the ineptness of automated image processing tools under heterogeneous (mixed) traffic conditions, a semi-automated image processing tool was used to develop trajectory data (Vicraman et al. 2014). In improving the marginal noise in the developed trajectory data, smoothening techniques were used (Venthuruthiyil and Chunchu 2018; Raju et al. 2017). For better readability, the details of the selected study section's trajectory data are presented in Table 1. The selected study sections' snapshots followed by the developed time–space plots of vehicles observed during real field conditions on the western expressway are shown in Figure 2. Six dominant vehicle categories were observed over the selected road sections: Motorized three-wheelers, Motorized two-wheelers, Buses, Cars, Trucks, and Light commercial vehicles (LCV).

Table 1. Details of the study section.

Study section	Trap length (m)	Road width (m)	Traffic flow classification	Traffic composition[a]	Traffic flow parameters			No. of vehicles tracked	Duration of trajectory data (minutes)
					Avg. speed (kmph)	Avg. flow PCU/h	V/C		
Western Express-way (Multilane Urban Roads)	120	17.5	Flow-1	15/35/5/40/2/3	65	4800	0.4	1080	15
			Flow-2	20/29/2/45/1/3	42	10120	0.85	1715	15
			Flow-3[b]	17/25/5/45/3/4	20	3500	< 1	660	10

[b]Stop and go conditions.
[a]Traffic composition in order of motorized three-wheelers/motorized two-wheelers/bus/car/truck/LCV.
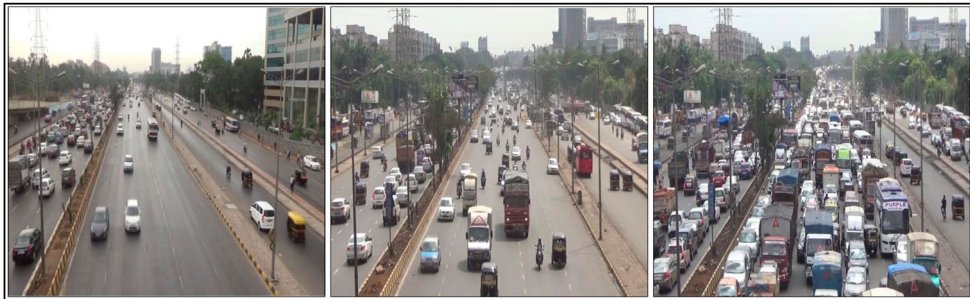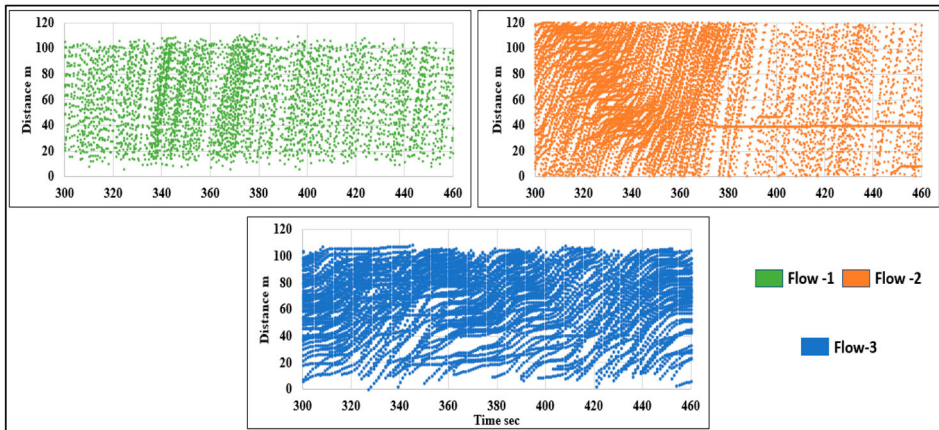
Figure 2. Snapshots of the study section (top) and time-space plots of vehicles (bottom) on the western expressway for different flow levels.

Modeling driving behavior

Under mixed-traffic conditions, the presence of different vehicle categories and the ensuing weak lane discipline inevitably results in numerous complex interactions. As a result, even the well-established car-following and lane-change models may not be directly used in modeling such conditions. As such, various driving behavior-related parameters are not adequately studied for such conditions. For example, consider two vehicles are interacting in a traffic stream (leader–follower pair), let the leader be relatively slower than the follower. Under homogeneous lane-disciplined traffic, the follower vehicle will match the leader vehicle speed and tends to change the lane to have a comfortable movement. However, in the case of mixed-traffic conditions with non-lane-based traffic behavior, given the same

scenario, the subject vehicle will most likely shift laterally for its comfort to pass its leader vehicle. The extent of the subject vehicle's lateral movement depends on the surrounding vehicles present in the stream and the lateral freedom available for maneuvering. This unique phenomenon under mixed-traffic conditions can be attributed to the car-following models' low performance for lane-based conditions. Such models cannot explain the longitudinal movement in combination with lateral shifting simultaneously.

To address the research gap, a driving behavior logic was developed to model driving behavior under mixed-traffic conditions. Instead of discretizing the following and lane-change behavior as homogeneous traffic conditions, the selected car-following models were adapted, where the subject vehicle is mostly influenced by the surrounding vehicles present in its surrounding zone.

Consider a leader–follower vehicle pair in a mixed traffic stream, having a longitudinal space of y, and the center of the follower is shifted to the right concerning the center of the leader (lateral shift) with a distance L, as shown in Figure 3. Let Lc be the comfortable lateral distance of the subject vehicle to pass its leader vehicle. When the leader vehicle is comparatively moving slower than its subject (less than the subject's desired speed) as a result of mixed traffic conditions, the subject vehicle tends to move in either to the left or to the right of the subject vehicle with angles α or β, respectively, as shown in Figure 3. With the availability of lateral freedom, the probability that the subject vehicle selects the right movement with a lesser angle β is higher than selecting the left movement with a higher angle α. Considering this phenomenon, both lateral and following behaviors of vehicles will be formulated in the same model. The angles α or β are given by

$$\alpha = \tan^{-1}\left[\frac{L + Lc + 0.5w_L}{y}\right] \tag{1}$$

$$\beta = \tan^{-1}\left[\frac{L + Lc - 0.5w_L}{y}\right] \tag{2}$$

where w_L is the width of the leader vehicle. The angle of the subject vehicle for preferred longitudinal movement, θ, is given by

$$\theta = \min\{|\alpha|, |\beta|\} \tag{3}$$

On the other hand, with various surrounding vehicles in the picture, the behavior of the subject vehicle can be miscalculated by considering only a single leader vehicle. To better understand the vehicular movement phenomenon, traffic-flow movements over the road section were thoroughly observed. It was found that the subject vehicle is mainly influenced by its surrounding vehicles, and it tends to come out of its surrounding vehicles and laterally move to any available space on the road. This behavior is illustrated in Figure 4 by the locations of the subject vehicle (motorized two-wheeler, marked in yellow) over different time frames.

Considering the above phenomenon in Figure 4, it was planned to identify the surrounding vehicles over the subject vehicle, for this a surrounding zone of length 'l' and width 'm' for a subject vehicle was specified as shown in Figure 5. Based on this premise, five possible combinations of surrounding vehicles can be identified in the present study for a given subject vehicle. Figure 5 depicts the surrounding vehicle designations as leading and adjacent along with their relative sides based on their respective position concerning the subject vehicle.

Based on the type of vehicles in the surrounding zone, there can be potential five different surrounding vehicles with 24 combinations. Note that the scenario in Figure 3 is explained only for a single leader–follower pair with a lateral shift where the vehicle acquires the minimum angle when the subject vehicle is experiencing a delay. Based on the observed phenomenon in Figure 4, when the subject vehicle faces the discomfort of not having its desired speed due to the surrounding vehicles, it tends to move away from its surrounding vehicles. Based on the combination of the surrounding vehicles, the direction of the subject vehicle at that instant is specified so that when the vehicle is not moving at its desired speed, it tends to switch its lateral position over the road space. When the subject
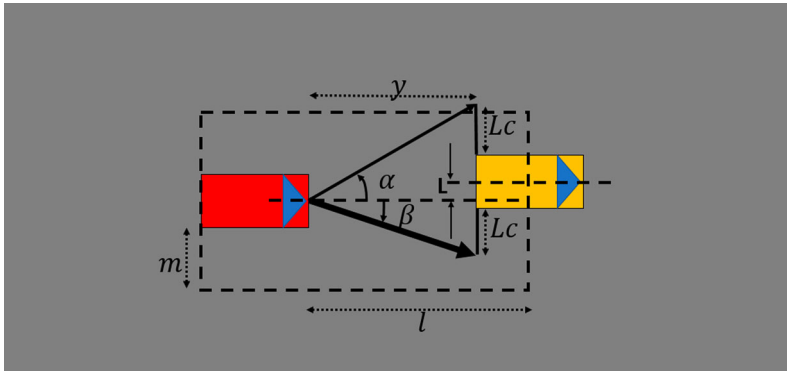
Figure 3. Concept of angular longitudinal movement of the subject follower vehicle.
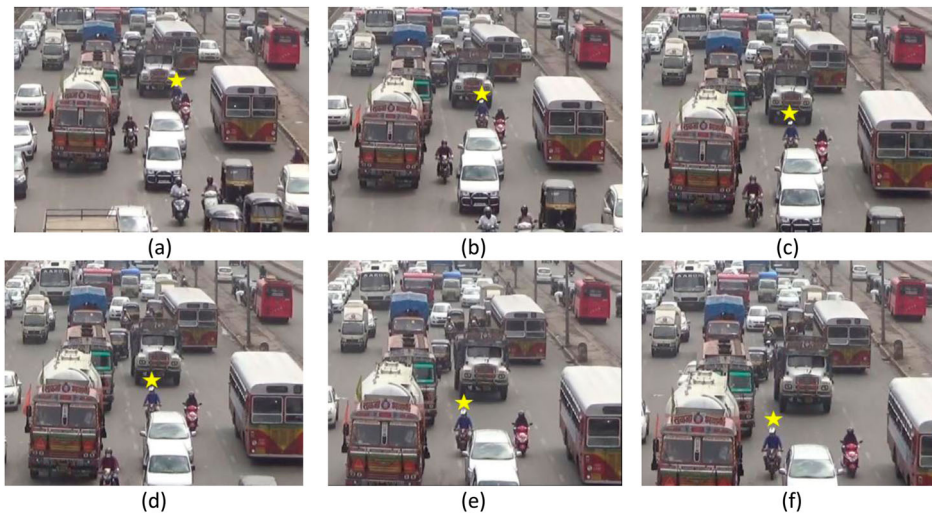
Figure 4. Subject vehicle locations in the traffic stream (highlighted) in different time frames.

is not having any surrounding vehicles, it tends to move at its desired speed. When only the leader is ahead, the subject vehicle finds the minimum angle for movement. Furthermore, the subject finds the appropriate gap to pass those vehicles with the surrounding and leader vehicles. Based on the combination of vehicles in the surrounding zone of the subject vehicle, the preferred direction of movement (shown as a bold arrow) is explained in Figure 6.

Discussion on car-following model selection

Numerous car-following and lane-changing behavior models were reported in the literature (Pourabdollah et al. 2017; C. Chen et al. 2010; Yang et al. 2018). It was observed that both Intelligent Driving Model (IDM) and Gipps model are reported as one of the robust models in modeling traffic conditions. A few researchers (Milanés and Shladover 2014; X. Chen et al. 2010) reported that the IDM could model autonomous vehicles. Considering their performance in modeling driver behavior and their robust mathematical formulation, both IDM and Gipps models are chosen in the present study to model driver behavior in mixed-traffic flow conditions.

(a) With surrounding vehicles

(b) marking the surrounding vehicles

(c) Labelling the surrounding vehicles
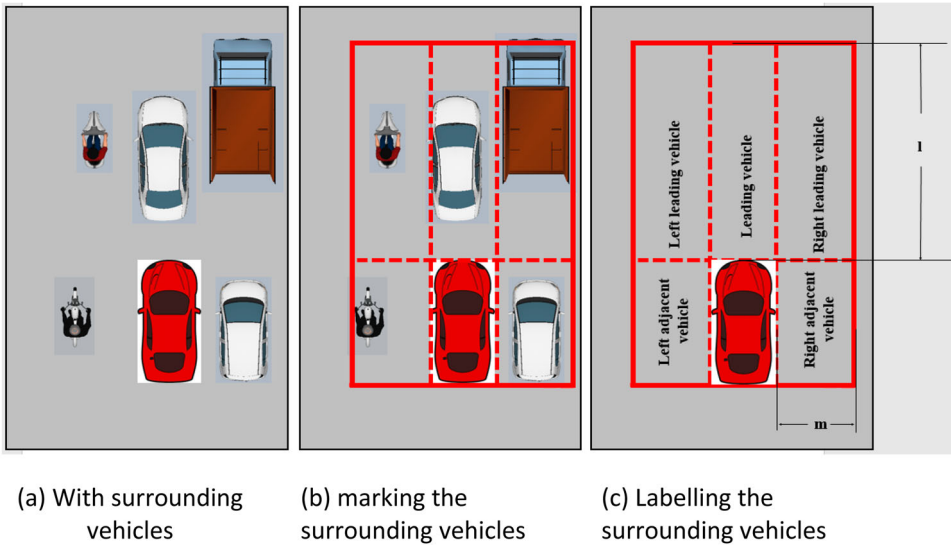
Figure 5. Identification of surrounding vehicles for the subject vehicle.
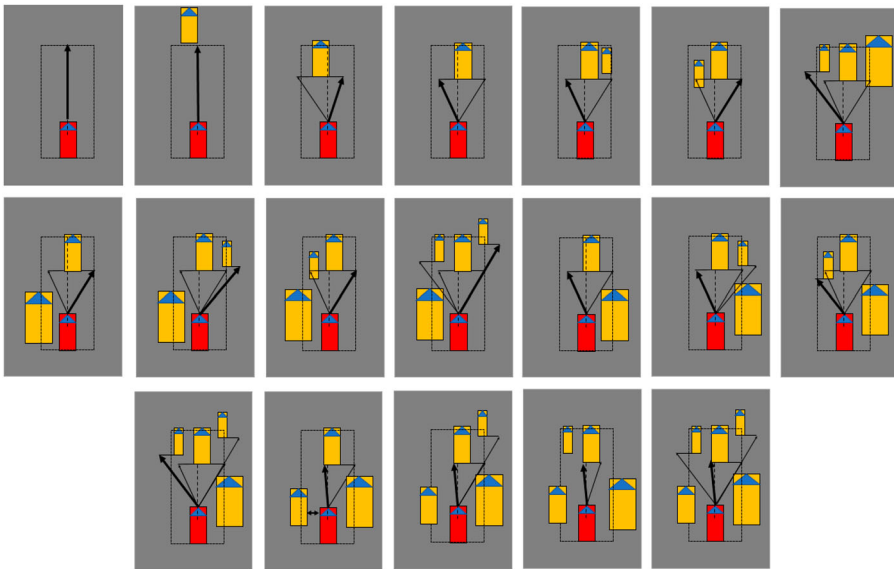
Figure 6. Preferred direction of the subject vehicle in combination with surrounding vehicles.

Intelligent driving model (IDM)

To model the behavior of vehicles, Treiber, Hennecke, and Helbing (2000) proposed the IDM. In addition, numerous studies adopted the IDM for modeling prevailing traffic conditions (Derbel et al. 2013; Derbel et al. 2018; Eggert, Damerow, and Klingelschmitt 2015; Laquai et al. 2013). In general, the IDM expresses the acceleration of a subject vehicle as a function of its desired maximum acceleration. Based on the subject vehicle's current speed and available gap with its leader vehicle, the desired maximum acceleration of the vehicle is estimated in such way that the vehicle attains its desired speed under free-flow traffic conditions and avoids collision by restricting its acceleration to maintain a minimum safe

gap with its leader vehicle. Let the following variables of the subject vehicle be denoted as: desired maximum acceleration of vehicle a_{max}, speed v, desired speed V, tentative minimum gap S_{min}, and distance gap between the leader and subject vehicles S.

Thus, the acceleration of the subject vehicle a is given as

$$a = a_{max} \times \left[1 - \left(\frac{v}{V} \right)^{\delta} - \left(\frac{S_{min}}{S} \right)^2 \right] \tag{4}$$

The minimum desired gap among the vehicles S_{min} at jam conditions is given by

$$S_{min} = s_0 + s_1 \sqrt{\frac{v}{V}} + Tv + \frac{v \Delta v}{2\sqrt{a_{max}b}} \tag{5}$$

where δ is the acceleration parameter, s_0 is the gap at jam conditions, s_1 is the gap factor, T is the reaction time of driver, and b is the comfortable deceleration (positive value). Then, based on the core logic formulation of IDM, the boundary conditions are assessed as follows

$$\text{when } \begin{Bmatrix} v \to V \\ S \to null \end{Bmatrix} \quad a = 0 \tag{6}$$

$$\text{when } \begin{Bmatrix} v \to 0 \\ S \to null \end{Bmatrix} \quad a = a_{max} \tag{7}$$

$$\text{when } \begin{Bmatrix} v < V \\ S > S_{min} \end{Bmatrix} \quad a < b \tag{8}$$

$$\text{when } \begin{Bmatrix} v < V \\ S \to S_{min} \end{Bmatrix} \quad a = b \tag{9}$$

From the preceding formulation, it noted that the acceleration of a subject vehicle is quantified in such a way that the vehicle always tends to maintain the desired speed V under free-flow conditions and decelerates to avoid the minimum gap S_{min} from its leader vehicle. As per IDM, the acceleration of the subject vehicle is accessed based on the speed ratio (v/V) and the distance gap ratio (S_{min}/S) for the longitudinal movements of the vehicles.

Gipps model

Another potential model, named the Gipps model(Gipps 1981), was considered to model mixed-traffic behavior. Unlike IDM, the Gipps model is a multi-regime model, conceptualized based on maintaining a safe time gap from the leader vehicle. Some studies modified the classical Gipps model for modeling prevailing traffic conditions (Gunay 2007; Yang et al. 2013; Papathanasopoulou and Antoniou 2015). In general, the following behavior of vehicles is expressed using two phases (acceleration and deceleration), and the driver's response is quantified accordingly. The basic concept involved in the model is that when the subject vehicle is not under the influencing zone of the leader vehicle, the subject vehicle tends to maintain its desired speed using acceleration (modeled as acceleration phase). Whereas, if the subject vehicle is under the influence of the leading vehicle, it tends to maintain a safe time gap from the leading vehicle through acceleration and deceleration. The desired speed constraint fitted from field data is given by

$$v(T) \leq v + 2.5 T a_{max} \left(1 + \frac{v}{V} \right) \sqrt{0.025 + \frac{v}{V}} \tag{10}$$

When the leading vehicle brakes to slow down, the speed limit that avoids collision was derived from the equation of motion as

$$v(T) \leq bT + \sqrt{b^2 T^2 - b[2(S_{min}) - vT - \frac{V}{b}]} \tag{11}$$

The boundary conditions of the Gipps model were evaluated as

$$\text{when } \begin{Bmatrix} v \to V \\ T \to 0 \end{Bmatrix} \quad v(T) = v \tag{12}$$

when $\{v \to 0\}$

$$v(T) = v + 2.5Ta_{max}\left(1 + \frac{v}{V}\right)\sqrt{0.025 + \frac{v}{V}};$$

$$v(T) = 2.5Ta_{max}\sqrt{0.025};$$

$$v(T) = 0.4Ta_{max}$$

$$v(T) = a_{max} \times \text{update interval} \quad (T = 2.5 \text{ s}) \tag{13}$$

$$\text{when } \begin{Bmatrix} v < V \\ S > S_{min} \end{Bmatrix} v(T) \leq bT \tag{14}$$

$$\text{when } \begin{Bmatrix} v < V \\ S \to S_{min} \end{Bmatrix}$$

$$v(T) = bT + \sqrt{b^2T^2 - b[2(S_{min}) - vT - \frac{V}{b}]} \tag{15}$$

$$v(T) = bT + \sqrt{b^2T^2 - b\left[2\left(vT + \frac{1}{2}aT^2\right) - vT - \frac{V}{b}\right]}, \left[S = vT + \frac{1}{2}aT^2\right]$$

$$v(T) = bT + \sqrt{b^2T^2 - b\left[2\left(\frac{1}{2}bT^2\right)\right]}, \text{ [as } S \to S_{min}; v \to 0 \text{ and } a \to b]$$

$$v(T) = bT + \sqrt{b^2T^2 - b^2T^2]}, \text{ [as } \quad S \to S_{min}; b \to max \text{ (to avoid collision)]}$$

$$v(T) = bT \tag{16}$$

From the boundary conditions, the speed of a subject vehicle is given under a multi-regime formulation. For example, under free flow, the subject vehicle tends to maintain its desired speed V, with acceleration as a function of the speed ratio. On the other hand, when the subject vehicle experiences the stimulus of other leader vehicles, it is zoned in either of the two regimes, such that the subject vehicle maintains a minimum safe time gap from the leader vehicle. In this case, S_{min} plays a major role in deciding the safe time gap.

Inducing the angular logic

Both IDM and Gipps car-following models can be used to replicate mainly the longitudinal movement of vehicles. However, under mixed-traffic conditions, driving behavior is a combination of both simultaneous longitudinal and lateral behavior as a discretely continuous phenomenon. Hence, applying these models directly may not precisely incorporate mixed traffic behavior. Therefore, in this study, the hypothesized behavioral logic of these two car-following models was adopted for modeling mixed-traffic behavior.

To describe the logic in a better manner, two vehicles are considered, as shown in Figure 7. Let Lc be the comfortable lateral distance between the vehicles to have a passing movement for the subject, L be the lateral shift between the vehicles, and L/Lc be the clearance ratio. When the clearance ratio is less

than 1, the subject vehicle must be under the influence of its leader vehicle and respond accordingly. On the other hand, a clearance ratio equal to or greater than 1 signifies the availability of freedom for lateral movement, in which the subject vehicle can pass its leader vehicle instead of the lane change, as shown in Figure 7. Even with multiple surrounding vehicles, Lc is calculated similarly. Therefore, the classical car-following models were adapted to model the lateral behavior and thus replicate driving behavior under mixed-traffic conditions more realistically.

Customizing IDM model

To induce the lateral behavior logic in the IDM, once again the formulation of IDM was examined. To induce lateral behavior, it was envisioned to customize the IDM model. Along with v/V and S_{min}/S factors, for mimicking lateral behavior, L/L_c was introduced in the IDM model. To sensitize the lateral behavior an exponent factor β was given to L/L_c, which acts almost like δ in v/V. On these lines, the newly customized IDM for an ideal passing behavior is given as Equations (17) and (18).

$$a = a_{max} \times \left[1 - \left(\frac{v}{V} \right)^{\delta} - \left(\frac{S_{min}}{S} \right)^{2} + \left(\frac{L}{L_c} \right)^{\beta} \right] \tag{17}$$

Again, it can be implied that the factor L/L_c should not active over the entire simulation time, otherwise will result in desired maximum for the subject vehicle in most of the times. At the same time, L/L_c should be activated when the subject vehicle is having lateral freedom to pass the surrounding leader vehicles, instead of following them. Considering this in the present work, a dummy coefficient 'ω' was factored to L/L_c. Whereas ω takes the values of either unity or zero based on the availability of lateral freedom to the surrounding vehicles. On the lines, customized IDM is given as

$$a = a_{max} \times \left[1 - \left(\frac{v}{V} \right)^{\delta} - \left(\frac{S_{min}}{S} \right)^{2} + \omega \left(\frac{L}{L_c} \right)^{\beta} \right] \tag{18}$$

$$\text{If } a > a_{max} \text{ then } a = a_{max} \tag{19}$$

On these lines, the boundary conditions of the customized IDM were evaluated as shown in Table 2.
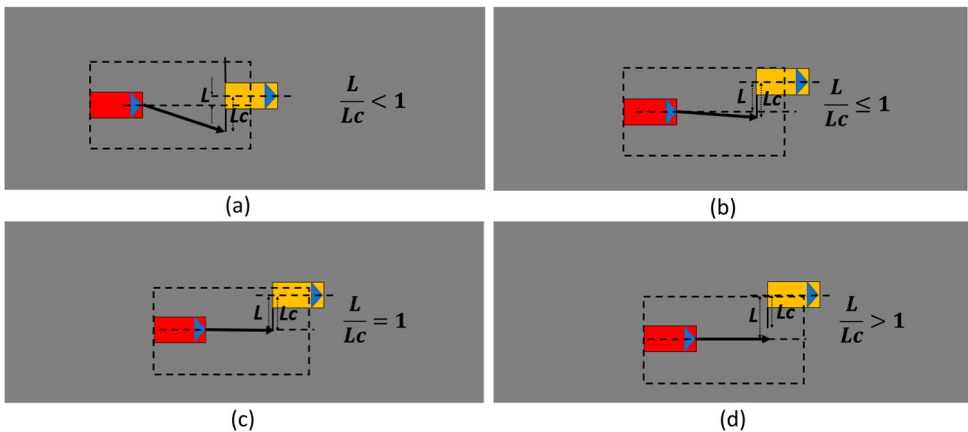

Figure 7. Behavior of subject vehicle at different scenarios.

Table 2. Boundary conditions of customized IDM over different scenarios.

Boundary condition	Acceleration of the vehicle	Inference
$\begin{cases} v \to V \\ S \to null \\ L \to null \end{cases}$	$a = 0;$	Vehicle in free flow conditions
$\begin{cases} v \to 0 \\ S \to null \\ L \to null \end{cases}$	$a = a_{max};$	Vehicle is about to start from stoppage conditions.
$\begin{cases} v < V \\ S > S_{min} \\ L \to null \end{cases}$	$a = a_{max} \times \left[1 - \left(\frac{v}{V}\right)^{\delta} - \left(\frac{S_{min}}{S}\right)^{2} \right] b < a < a_{max};$	Vehicle is under the influence of the leader.
$\begin{cases} v < V \\ S \to S_{min} \\ L \to null \end{cases}$	$a = a_{max} \times \left[-\left(\frac{v}{V}\right)^{\delta} \right]$ $a > b;$	Stopping conditions and vehicles having lateral freedom.
$\begin{cases} v < V \\ S \to S_{min} \\ L < L_{c} \\ \omega \to 0 \end{cases}$	$a = a_{max} \times \left[-\left(\frac{v}{V}\right)^{\delta} \right]$ $a > b;$	Stopping conditions and vehicles not having lateral freedom.
$\begin{cases} v < V \\ S \to S_{min} \\ L \to L_{c} \\ \omega \to 1 \end{cases}$	$a = a_{max} \times \left[-\left(\frac{v}{V}\right)^{\delta} + 1 \right] 0 < a < a_{max}$	Stopping conditions, but the vehicle having lateral freedom, due this vehicle switches the lateral position and maintains its speed.
$\begin{cases} v < V \\ S \to S_{min} \\ L > L_{c} \\ \omega \to 1 \end{cases}$	$a = a_{max} \times \left[1 - \left(\frac{v}{V}\right)^{\delta} + \left(\frac{L}{L_{c}}\right)^{\beta} \right] 0 < a < a_{max}$	Vehicle switches its lateral position and passes over its surrounding vehicles.
$\begin{cases} v < V \\ S \to S_{min} \\ L > L_{c} \\ \omega \to 0 \end{cases}$	$a = a_{max} \times \left[-\left(\frac{v}{V}\right)^{\delta} \right] a > b$	Vehicle follows its leader vehicle and computes position based on traditional IDM formulation.
$\begin{cases} v < V \\ S \to S_{min} \\ L > L_{c} \\ \omega \to 1 \end{cases}$	$a = a_{max} \times \left[1 - \left(\frac{v}{V}\right)^{\delta} - \left(\frac{S_{min}}{S}\right)^{2} + \left(\frac{L}{L_{c}}\right)^{\beta} \right] b < a < a_{max}$	Vehicle follows its leader vehicle and computes position based on new customized IDM formulation.

It can be noted that customized IDM, with the induced lateral behavior of vehicles, the sense of the IDM has not been changed under normal conditions, additionally at the same time with lateral behavior in the picture, it is also able to handle mixed-traffic sense reasonably well.

Customizing Gipps model

Like IDM, Gipps model was tweaked to model the mixed traffic conditions. As Gipps was multi regime car following model, in the present case it was sensed that lateral behavior comes when the vehicle is nearing its safety distance, considering this only the safety distance part of the Gipps was tweaked. It was noticed that safety distance part consists of deceleration factors, given the scenario of vehicle having the lateral freedom at near safety distance conditions, the subject vehicle should not be complete deceleration phase. To cater this, maximum acceleration a_{max} was factored with L/L_c. Like IDM again dummy coefficient 'ω' and exponent factor 'γ' was conceptualized. Based on this the final customized Gipps model is given as in equations 20 and 21

$$v(T) \leq v + 2.5 T a_{max} \left(1 + \frac{v}{V} \right) \sqrt{0.025 + \frac{v}{V}} \qquad (20)$$

Table 3. Boundary conditions of customized Gipps model over different scenarios.

Boundary condition	Velocity of the vehicle	Inference
$\begin{cases} v \to V \\ S \to null \\ L \to null \end{cases}$	$v(T) = V$	Vehicle in free-flow conditions
$\begin{cases} v \to 0 \\ S \to null \\ L \to null \end{cases}$	$v(T) = v + 2.5Ta_{max}\left(1 + \dfrac{v}{V}\right)\sqrt{0.025 + \dfrac{v}{V}};$ $v(T) = 2.5Ta_{max}\sqrt{0.025};$ $v(T) = 0.4Ta_{max}$ $v(T) = a_{max} \times$ update interval; [T = 2.5 s]	Vehicle is about to start from stoppage conditions.
$\begin{cases} v < V \\ S > S_{min} \\ L \to null \end{cases}$	$v(T) = v + 2.5Ta_{max}\left(1 + \dfrac{v}{V}\right)\sqrt{0.025 + \dfrac{v}{V}}$	Vehicle is under the influence of the leader.
$\begin{cases} v < V \\ S \to S_{min} \\ L \to null \end{cases}$	$v(T) = \text{Min}\begin{cases} v + 2.5Ta_{max}\left(1 + \dfrac{v}{V}\right)\sqrt{0.025 + \dfrac{v}{V}} \\ bT + \sqrt{b^2T^2 - b\left[2(S_{min}) - vT - \dfrac{V}{b}\right]} \end{cases}$	Stopping conditions and vehicles having lateral freedom.
$\begin{cases} v < V \\ S \to S_{min} \\ L < L_c \\ \omega \to 0 \end{cases}$	$v(T) = bT + \sqrt{b^2T^2 - b\left[2(S_{min}) - vT - \dfrac{V}{b}\right]}$	Stopping conditions and vehicles not having lateral freedom.
$\begin{cases} v < V \\ S \to S_{min} \\ L \to L_c \\ \omega \to 1 \end{cases}$	$v(T) = bT + \sqrt{b^2T^2 - b\left[2(S_{min}) - vT - \dfrac{V}{b}\right]} + a_{max}T\left(\dfrac{L}{L_c}\right)^{\gamma}$	Stopping conditions, but the vehicle having lateral freedom, due this vehicle switches the lateral position and maintains its speed.
$\begin{cases} v < V \\ S \to S_{min} \\ L > L_c \\ \omega \to 1 \end{cases}$	$v(T) = \text{Min}\begin{cases} v + 2.5Ta_{max}\left(1 + \dfrac{v}{V}\right)\sqrt{0.025 + \dfrac{v}{V}} \\ bT + \sqrt{b^2T^2 - b\left[2(S_{min}) - vT - \dfrac{V}{b}\right]} + a_{max}T\left(\dfrac{L}{L_c}\right)^{\gamma} \end{cases}$	Vehicle switches its lateral position and passes over its surrounding vehicles.
$\begin{cases} v < V \\ S \to S_{min} \\ L > L_c \\ \omega \to 0 \end{cases}$	$v(T) = \text{Min}\begin{cases} v + 2.5Ta_{max}\left(1 + \dfrac{v}{V}\right)\sqrt{0.025 + \dfrac{v}{V}} \\ bT + \sqrt{b^2T^2 - b\left[2(S_{min}) - vT - \dfrac{V}{b}\right]} \end{cases}$	Vehicle follows its leader vehicle and computes position based on traditional Gipp's formulation.

The velocity limitation that can avoid collision, when the leading vehicle brakes to slow down was derived from the equation of motion given as

$$v(T) \leq bT + \sqrt{b^2T^2 - b\left[2(S_{min}) - vT - \frac{V}{b}\right]} + a_{max}T\omega\left(\frac{L}{L_c}\right)^{\gamma} \tag{21}$$

On these lines, the boundary conditions of the tweaked Gipps model were evaluated as shown in Table 3.

Similarly, with the inclusion of lateral behavior in the model (based on the boundary conditions) it is noted that, the sense of the classical Gipps model did not actually change for the longitudinal movement. Rather, the customized Gipps model can handle the lateral behavior of the vehicles more realistically. Furthermore, it can be noted that ω plays a key role in activating the lateral importance in the Gipps model and will be equal to either 0 or 1. Thus, the lateral movement is activated in the model only when the subject vehicle has lateral freedom to pass its surrounding vehicles to the left or to the right to attain its desired speed, where $\omega = 1$. When the subject vehicle is surrounded by the

Table 4. Direction of the follower vehicle for different surrounding vehicle combinations.

Vehicles presence in surrounding zone						
Left leading vehicle	Leading vehicle	Right leading vehicle	Left adjacent vehicle	Right adjacent vehicle	ω	Direction of follower vehicle at that instant
No	No	No	No	No	1	Straight movement
No	Yes	No	No	No	1	Direction to the left or right based on a minimum angle
No	Yes	Yes	No	No	1	Direction to the left of leader, irrespective of angle.
Yes	Yes	No	No	No	1	Direction to the right of leader, irrespective of angle.
Yes	Yes	Yes	No	No	1	Direction to the left or right, based on minimum angle to the left adjacent or right adjacent leading vehicles.
No	Yes	No	Yes	No	1	Direction to the right of leader, irrespective of angle.
No	Yes	Yes	Yes	No	1	Direction to the right, based on right adjacent leading vehicles.
Yes	Yes	Yes	Yes	No	1	Direction to the right, based on right adjacent leading vehicles.
No	Yes	No	No	Yes	1	Direction to the left of leader, irrespective of angle.
No	Yes	Yes	No	Yes	1	Direction to the left of leader, irrespective of angle.
Yes	Yes	No	No	Yes	0	Direction to the left, based on left adjacent leading vehicles.
Yes	Yes	Yes	No	Yes	0	Direction to the left, based on left adjacent leading vehicles.
No	Yes	No	Yes	Yes	0	Direction to the left or right edge of the leader based on minimum angle
No	Yes	Yes	Yes	Yes	0	Direction to the left or right edge of the leader based on minimum angle
Yes	Yes	No	Yes	Yes	0	Direction to the left or right edge of the leader based on minimum angle
Yes	Yes	Yes	Yes	Yes	0	Direction to the left or right edge of the leader based on minimum angle

vehicles and does not have freedom to pass, $\omega = 0$. The direction of the follower vehicle for different surrounding vehicle combinations are presented in Table 4.

Further, it can be noted that, in the case of both IDM and Gipps models, the variables s, V, L and ω are dependent on each other. It can be noted that both the models are originated by the presence of velocity. With the presence of *V*, the distance gap *S* comes into the picture. When the distance gap is approaching its minimum gap, the lateral distance *L* will be computed. Further based on the presence of lateral freedom, the presence of ω gets incorporated in the models. Due to this, the conventional number of combinations is not observed in Tables 2 and 3. In view of this, based on the model formulations, in the case of IDM and Gipps, about 9 and 8 combinations are observed, respectively.

Calibration of customized driving behavior models

The customized IDM and Gipps models are to be calibrated using data from actual field conditions to model the mixed-traffic flow behavior. Afterwards, the calibrated model parameters are to be assessed for their effectiveness. Furthermore, to compute the parameters, the surrounding vehicles for a given subject vehicle are to be identified. In the present work based on the developed vehicular trajectory data; program was coded using a tool, named MATLAB. With the help of available literature (Savolainen et al. 2012; Okuda, Sugie, and Suzuki 2018; Bärgman, Smith, and Werneke 2015), a surrounding zone of $l = 30$ m and $m = 2.5$ m, was specified and surrounding vehicles are identified at each instant of the time frame for the subject vehicle. Under homogeneous traffic conditions, where car-following models are mostly calibrated irrespective of the vehicle category. In the present case, considering the variation in driving behavior based on the change in the vehicle category, the driving behavior models are planned to calibrate individually for each vehicle category.

Table 5. Estimated parameters using trajectory datasets.

Parameters	Motorized three-wheelers	Motorized two-wheelers	Bus	Car	Truck	LCV
V(m/s)	15.49	19.91	16.81	17.98	15.69	15.91
S_{min}(m)	1.12	0.97	5.61	1.63	4.94	1.75
L_c (m)	0.65	0.52	1.46	1.21	1.68	0.97
a_{max} (m/s^2)	2.28	2.85	2.31	2.5	2.21	2.03
b(m/s^2)	−2.54	−2.94	−2.43	−2.59	−2.45	−2.23

Table 6. Calibrated parameters of models using optimization.

Model	Parameters	Motorized three-wheelers	Motorized two-wheelers	Bus	Car	Truck	LCV
IDM	δ	0.72	0.45	0.91	0.65	0.97	0.84
	β	0.65	1.12	0.31	0.94	0.23	0.51
Gipps	T	1.2	1.1	1.2	1.1	1.2	1.0
	γ	0.59	1.19	0.45	1.05	0.53	0.71

With the help of available trajectory from varied traffic volumes over the road sections under mixed-traffic conditions, vehicle-category wise common parameters in both the models such as V, S_{min}, L_c, a_{max} and b are evaluted directly form the trajectory data. Considering the error in taking extreme value, in the present case desired speed V is computed as 95th percentile velocities of vehicles, minimum gap S_{min} as 5 percentile of gaps, comfortable lateral clearance L_c is computed as average lateral clearance of vehicles with adjacent vehicles, maximum acceleration as a_{max} as 95th percentile value of accelerations and b as 95th percentile value of decelerations. Based on these the parameters are computed and reported in Table 5.

On the other hand, remaining parameters such as δ, β in IDM and T, γ in Gipps model cannot be evaluated directly from the trajectory sets and hence, needs to be optimized. To find the optimized values of these parameters Genetic algorithm was chosen based on the literature (Ranjitkar, Nakatsuji, and Kawamua 2005; Gurusinghe et al. 2002), initially, the models were coded in MATLAB optimization tool with the objective function of minimum error in the observed response and the modeled response. For IDM, the response is the acceleration of the vehicle, whereas, for Gipps, it is the vehicle's velocity. On this basis, optimization is repeated for numerous runs, till the variation among the calibrated parameters from the runs found to be minimum and the calibrated parameters are given in Table 6. To get the fine-tuned values, optimization runs were carried repetitively with a change in population size (range of 50– 500) and the number of stall generations (range of 1000– 10,000).

The evaluated parameters observed that smaller vehicles, namely motorized three-wheelers, car and motorized two-wheelers, tend to show some aggression in comparison to heavy vehicles. For example, they maintain higher desired speeds, less gap and less lateral share. Even from the optimized parameters in both the models, a similar inference was observed. For example, acceleration exponent δ of motorized two wheelers is 0.45 and bus is 0.91, for given v/V of 0.7 in both vehicles at free flow conditions. IDM gives 0.85 factor for motorized two-wheelers and 0.72 for bus, which signifies the aggressiveness of smaller vehicles even at higher velocities. Further, to sense the vehicle category-based behavior in the traffic stream, the factors of v/V, S_{min}/S and L/L_c are computed over different vehicle categories using trajectory data and their cumulative probability functions are presented in Figure 8.

For the speed ratio of Figure 8(a), it is noted that smaller vehicles (mainly motorized three-wheelers and motorized two-wheelers) tend to show high variation compared to other vehicle categories. That is, smaller vehicles tend to have higher acceleration than other vehicles at a given value of the speed ratio. On the other hand, heavy vehicles, as they approach their desired speeds, tend to maintain lesser acceleration values. For the distance gap ratio of Figure 8(b), the distributions of smaller vehicles are skewed towards the origin, which may be caused by their smaller S_{min} values. In the case of the clearance ratio of Figure 8(c), the variations were observed for heavy vehicles such as truck, bus, car, and
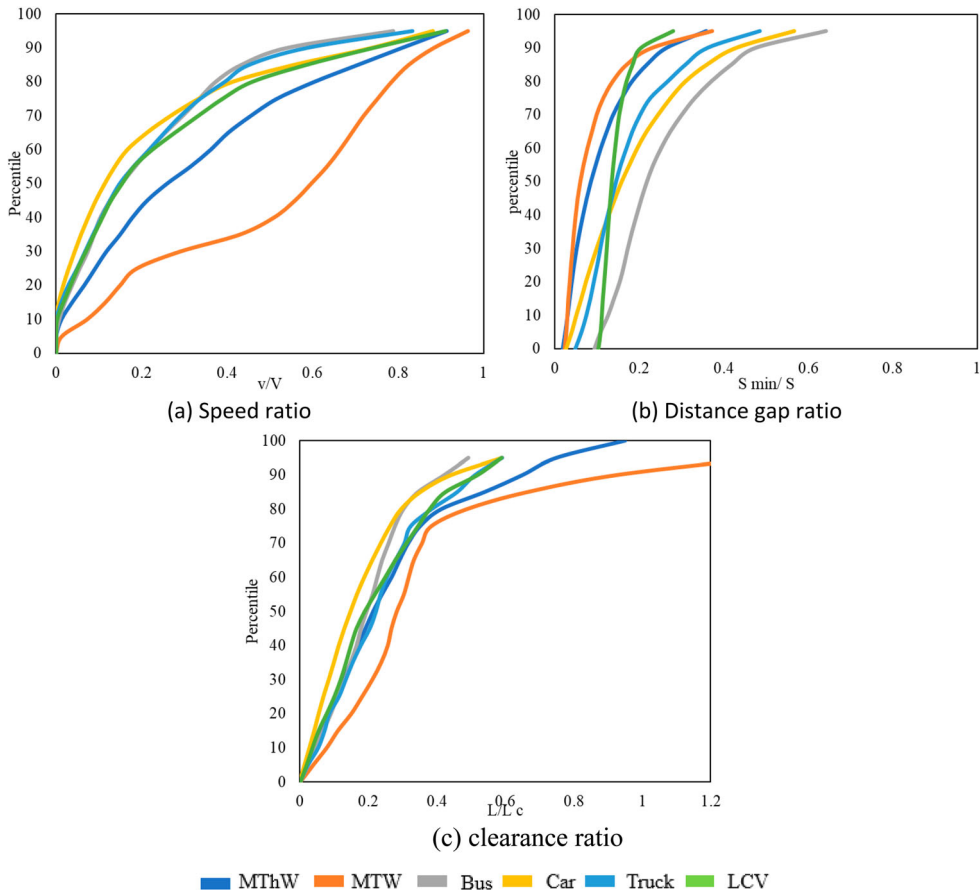
Figure 8. Cumulative probability functions of the speed, distance gap, and clearance ratios among different vehicle categories: (a) speed ratio, (b) distance gap ratio, and (c) clearance ratio.

LCV, where the ratios are in the range of 0–0.5. On the other hand, in the case of motorized three-wheelers and motorized two-wheelers, the values are in the range of 0–1.2, signifying the availability of lateral freedom for these vehicles traffic stream. These results indicate the underperformance of classical car-following models in mixed-traffic conditions.

Simulation modeling

Further, to comprehend customized driving behavior models' performance, it was planned to simulate the mixed traffic based on the models. Based on the literature (Rakha and Wang 2009; Brackstone and McDonald 1999; Rakha and Crowther 2002), it was noted that simulation is performed based on mathematical computations, where the calibrated models are numerically integrated with time to develop the speed–density relationship. On this basis, macroscopic fundamental traffic characteristics can be studied with the help of calibrated models. Nevertheless, to understand the logic of calibrated models in a sensible way, it was planned to employ the microscopic traffic simulation tools in the present work. Based on the author's previous experiences, in the present work microsimulation tool, PTV VISSIM, 11.0, was selected to model the traffic. Given this, the simulation model was developed, and necessary inputs such as road geometry, vehicle inputs, vehicle dimensions, desired speeds based on vehicle category were given as inputs to the simulation models.

In VISSIM, for driving behavior modeling, Wiedemann's psychophysical models (Wiedemann 1974) are used to replicate the following behavior and linear lateral share relationship with longitudinal velocity for inducing lateral behavior. Whereas to model the mixed traffic with customized driving models, these models have to be coded externally, for that in the present work, Application Program Interface module (API) (Vissim, 2018) was used to induce the customized driving behavior. In External Driver API, Dynamic Link Library (DLL) files are used as replacing the internal default behavior, the DLL files contain a Header file, which contains all the various libraries for the vehicle parameters and source file, in which the behavioral logic can be coded and the entire logic to be written in C++ platform.

To induce the framed concept of driving behavior in the microsimulation tool VISSIM the behavioral logic was coded so that, initially, the subject vehicle computes the surrounding vehicles in the surrounding zone. Based on the surrounding vehicle combination, the direction of the longitudinal movement will be assigned. With the selected value, the driving behavioral model will be activated, and the responses of the vehicle will be computed. Based on the responses, the position of the vehicles will be calculated as shown in Figure 9.

On the lines, it can be noted that as driving behavior was externally coded in VISSIM, initially due to some glitches/bugs in the code, some irrational behavior was observed and finally, by solving them, conceptualized behavioral logic was achieved in simulation. In giving due weightage to authors' efforts in achieving the process, some snapshots of these trials are presented in Figure 10 and simulation videos are presented in YouTube videos and URL-links for which are given in the Appendix at the end of this manuscript.
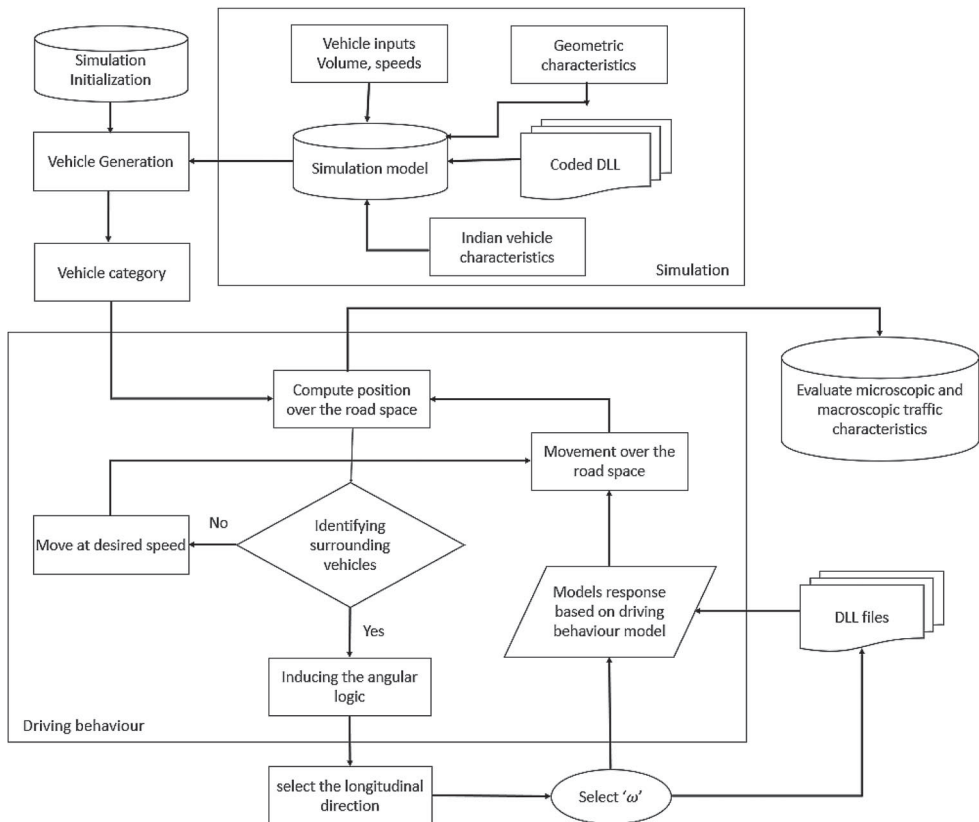

Figure 9. The logic of coding external driving behavior within the adapted models in VISSIM.
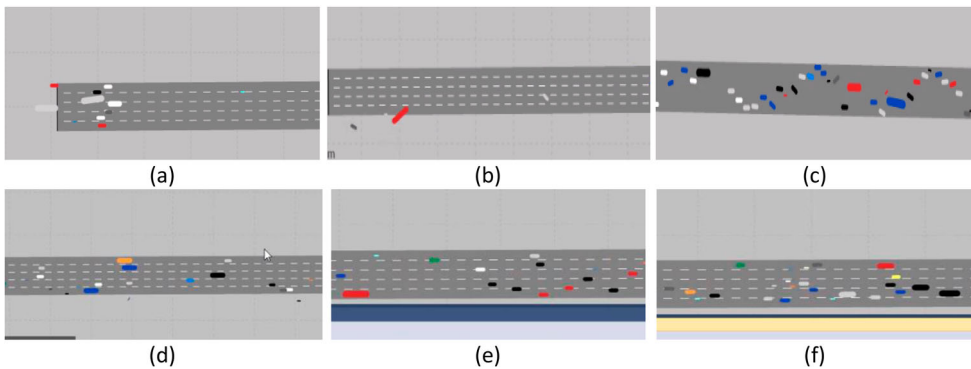
Figure 10. Selected snapshots of the simulation trials.

Behavior modeling: customized IDM

The conceptualized driving behavior logic was tested in VISSIM as per the simultaneous observations of different vehicular movements in longitudinal and lateral directions. The calibrated customized IDM was then coded using DLL source files, and simulation runs were performed. To study the calibrated customized IDM's performance comprehensively, simulation models are input with varying flow levels ranging from 1000 Vehicles/h to 13000 Vehicles/h with an interval of 500 Vehicles/h. To test the calibrated model's credibility comprehensively, vehicular trajectory data was developed from simulation models over varying flow levels, with a 5-minute sample at each of the flow levels varying over 100 min. Given this, longitudinal and lateral positions were noted for every 0.4 s and vehicle category for each vehicle. The value of 0.4 s was fixed based on the actual extracted trajectory data. To understand the microscopic interaction among the vehicles, Wiedemann's following concept was employed in the present work. The plots indicating distance gaps vs. relative velocities (follower minus leader) were made among the consecutive vehicles with any lateral overlap. It can be noted that vehicular pairs showing good behavior will result in a perfect or most ideal hysteresis phenomenon. Based on the developed trajectory data from simulation and the help of a MATLAB code, distance gap vs. relative velocity plots are developed. Based on the follower vehicle category, the plots are aggregated and overlaid with the hysteresis plots from field conditions shown in Figure 11. Further, for better clarity on the nature of variations, vehicle-category-wise relative velocity and distance gap distributions are also compared, as shown in Figure 11. The frequency distributions are shown above and at the right side of the relevant hysteresis plots.

In general, to understand the following behavior among the vehicles, Wiedemann (Wiedemann 1974) conceptualized a relationship between the distance gaps and the relative speeds among the vehicles. Based on this following behavior is modeled in different threshold regimes. In line with this, these two psychophysical following-behavior models (Wiedemann74 and 99) were developed. Based on this, even authors from their previous studies examined the driving behavior using hysteresis plots under India's mixed traffic conditions. It can be noted that when the follower vehicle is moving closer towards the leader, the distance gap will decrease. At some point, based on the follower vehicle responses, the follower vehicle will be under the regime of its leader. Given the reaction time and human (driver behavior) element, there will be a hysteresis phenomenon between the vehicles; on similar lines, when the leader is moving at a higher speed than its follower, the distance gap increases with an increase in the magnitude of relative speed. These traffic dynamics may be better comprehended using the following behavior among the vehicles. Hence, the hysteresis plots are studied taking different vehicle categories as following vehicles.

From the hysteresis (Figure 11), it is observed that plots from field conditions are more symmetric about the *y*-axis. On the other hand, with customized-IDM mainly at higher distance gaps, the plots
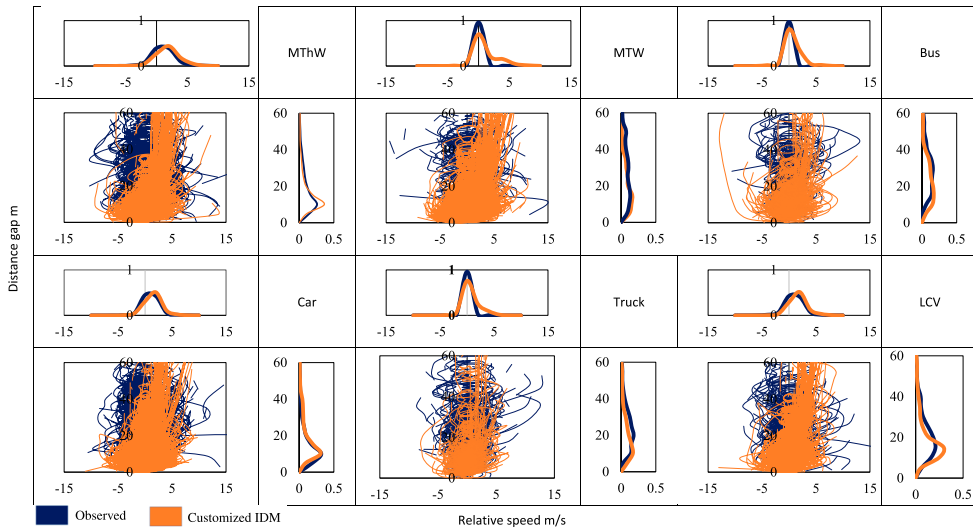
Figure 11. Comparison of hysteresis plots: Observed data and customized IDM data.

are found to be asymmetric, as the distance gaps decrease symmetry is increased, to understand this logic again customized IDM was inspected closely. It was identified that at higher distance gaps, the velocity of the subject vehicle is governed by only v/V with negligible values of S_{min}/S and L/L_c. As a result, the vehicle tends to be in acceleration phase to attain its desired velocity, due to which the data is skewed towards the right-side axis. Whereas, at less distance gaps, S_{min}/S and L/L_c gets into a major role and govern the vehicle instincts which results into hysteresis phenomenon among the vehicles and hence matches well with field observed hysteresis. This means that the modified parameters in IDM can replicate the observed driving behavior well for relative spacing ranging from 0 to 30 m. Nevertheless, it may be noted that any car-following model's performance, for example, customized IDM in this case, should be reasonably good, particularly in the following zone. The following zone considered here is based on the subject vehicle type and vehicles in surrounding of that.

Further, to assess the calibrated driving behavior model, simulation runs are performed, and speed–flow plots are developed, and the mixed-traffic was homogenized using appropriate PCU values (Kumar et al. 2018). Based on these, speed–flow plots are developed and overlaid over the observed plots, as shown in Figure 12. The macroscopic plots show that the calibrated customized-IDM replaces the traffic characteristics with less variation than observed data. The investigation on customized IDM reveals that, in general, customized IDM falls under a single regime formulation. In other words, it means that for a given gap, lateral overlap, and desired speed, it gives a unique value. As a result, less variation was observed in modeled data.

Behavior modeling: Classical IDM

In the present work, to understand the importance of angular logic, the simulation runs are performed with classical-IDM formulation, by calibrating the essential parameter δ and keeping ω as zero and similar to previous cases, hytsreisis plots are devloped. From the hysteresis plots, it is observed that the plots became slender compared to observed data plots. This shows that vehicles tend to behave in uniform (perfect-following behavior) nature, as shown in Figure 13. With the classical-IDM model, the subject vehicles are only responding to their leader vehicles and lateral displacements are not captured well. As discussed, due to its model formulation, consistency in driving behavior was observed in the simulation models.
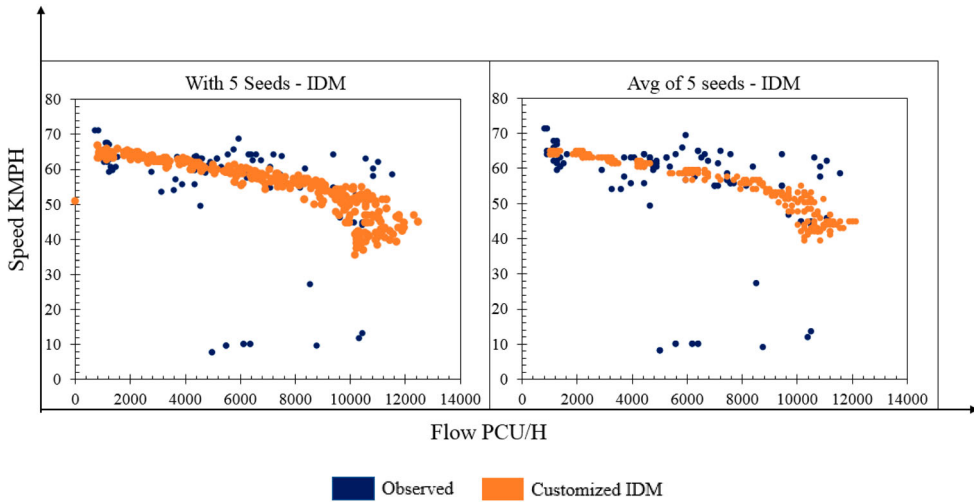
Figure 12. Comparison of speed flow plots: Observed data and customized IDM data.
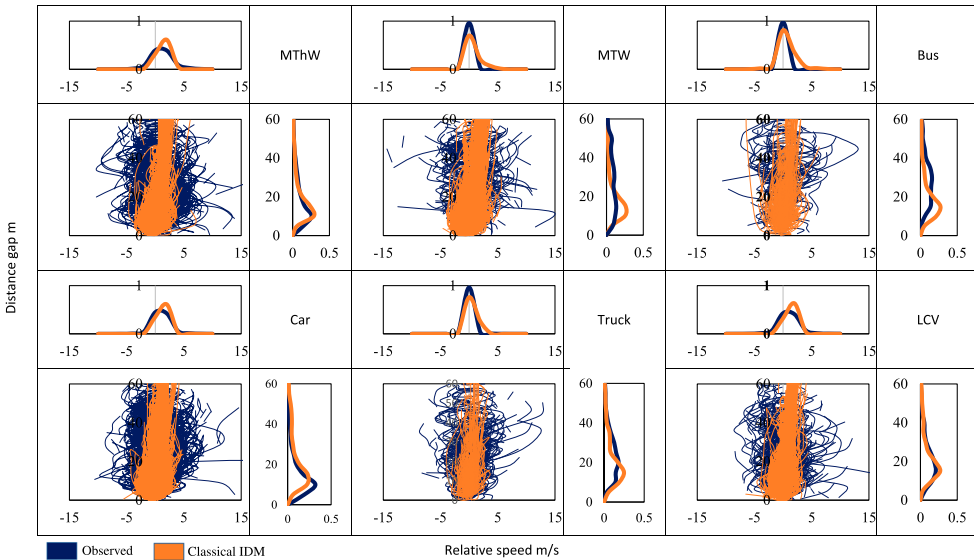

Figure 13. Comparison of hysteresis plots: Observed data and classical IDM data.

Furthermore, to understand the macroscopic traffic sense, macroscopic traffic plots are developed again, as shown in Figure 14. From the speed–flow plots, it is observed that adopting classical-IDM, the relationship tends to be in linear form and supports literature (Treiber, Hennecke, and Helbing 2000) in this direction. It can be attributed to uniformity in driving behavior (perfect-following behavior without lateral displacements). Due to this, even the capacity value is higher when compared with the capacity value found for actual field conditions.

Behavior modeling: customized GIPPS model

Like IDM, a customized Gipps model was induced in the simulation model through DLL files, and runs are carried out. To sense the model's performance trajectory data was captured from the simulation
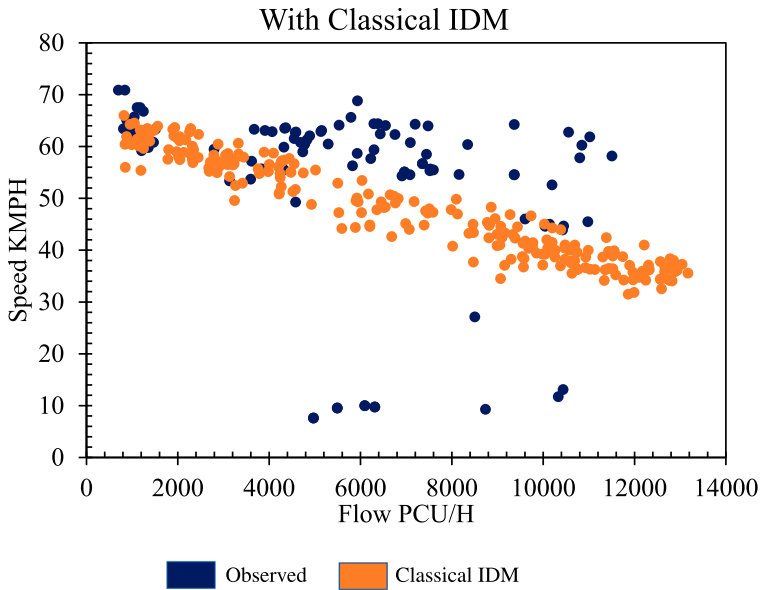
Figure 14. Comparison of speed flow plots: Observed data and Classical IDM data.

runs, and hysteresis plots are developed, as shown in Figure 15. From the plots, it was identified that, like IDM, even with the Gipps model at higher distance gaps, hysteresis plots tend to be asymmetric. On the other hand, at less distance gap, variations in relative velocities tend to be less, and plots become narrower, unlike IDM. It was inferred that as the Gipps model is a multi-regime formulation model with the concept of a safety time gap, as a result, similar to IDM at free-flow conditions, vehicles are in a free-flow regime. As distance gaps decrease, multi-regime formulation comes in to picture, resulting in symmetric plots. Whereas, at a safe time gap, the vehicles tend to match the leader velocity with constrained lateral freedom from the leader vehicles at less distance gap. As a result, variation in relative velocities is less in this zone, unlike in IDM model analysis.

Based on simulation runs adopting the customized-Gipps model, macroscopic traffic characteristics were evaluated, and speed–flow plots are developed, as presented in Figure 16. It is identified clearly that customized-Gipps models can cater to the variation of field data much reliably and indicate a better matching pattern than customized-IDM. The main reason, which can be attributed to this performance of the model, is again its multi-regime formulation logic, which can mimic the variation in flow at a macroscopic level, unlike single regime IDM.

Behavior modeling: classical GIPPS model

In the present work, to understand the importance of angular logic in Gipps model, again the simulation models are performed with classical Gipps model formulation, by calibrating the essential parameter γ and keeping ω as zero. Again, trajectory data was developed, hysteresis plots are evaluated and compared with the respective field data for all vehicle categories. From the plots, it may be noted that at lesser relative spacing, the hystersis plots are in slender in nature, as compared to higher distance gaps and with varied shape from customized-Gipps. From the visualization on hysteresis plots, in Figure 17, it may be inferred that at higher disance gaps, the subject vehicle tends to attain desired velocity, whereas when the distance gap decreases, vehicle will be in either in acceleration phase or deceleration phase. At a distance gap under a traffic condition, near to safe time gap, with inactive 'L/L_c' logic, the follower vehicle tends to match the leader vehicle, instead of passing it with aggrssive lateral movement behavior, as a result, hystersis plots are slender in this region.
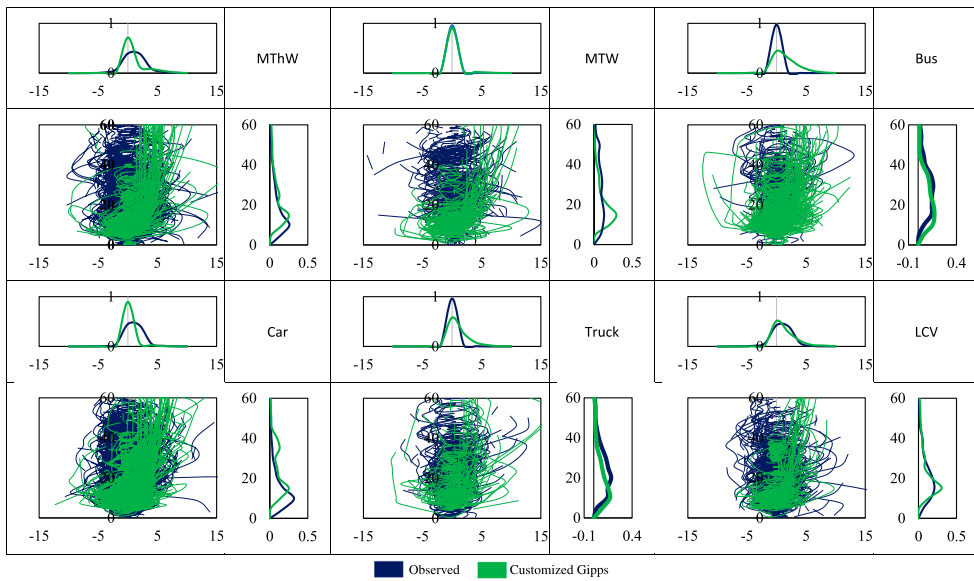
Figure 15. Comparison of hysteresis plots: Observed data and customized Gipps model data.
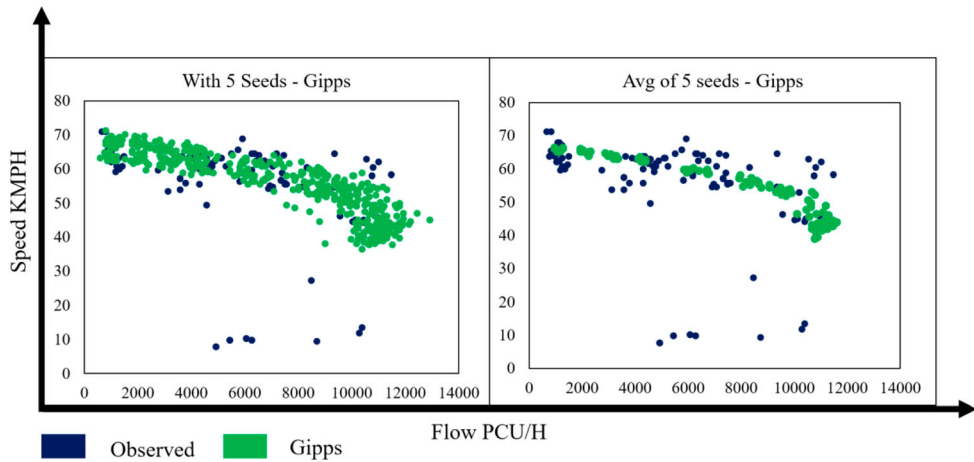
Figure 16. Comparison of speed–flow plots: Observed data and customized Gipps model results.

Based on the adopted framework, macroscopic plots are again developed using the classical Gipps model compared to the customized Gipps model. The speed–flow plots are depicted in Figure 18. It may be noted that the capacity value is found to be lesser, and the shape is slightly skewed in nature. At near-capacity conditions, aggressive lateral behavior plays a significant role in accommodating the number of vehicles, thereby increasing the capacity value. In the present case, with deactivated lateral inducing nature, it resulted in a drop in capacity and slightly changed the shape of the plot.

Results and discussions

Further to summarize the models' performance, statistical analysis has been carried out at the microscopic hysteresis level. Where relative velocity and distance gap distributions are compared among observed data and modeled data, the chi-square test was initially performed, and the *p*-values are
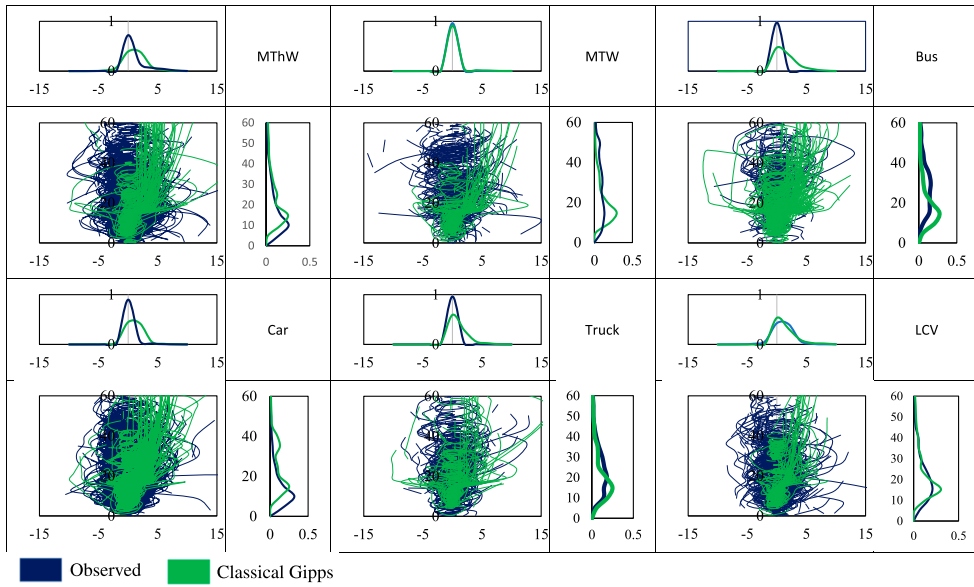
Figure 17. Comparison of hysteresis: Observed data and classical Gipps model results.
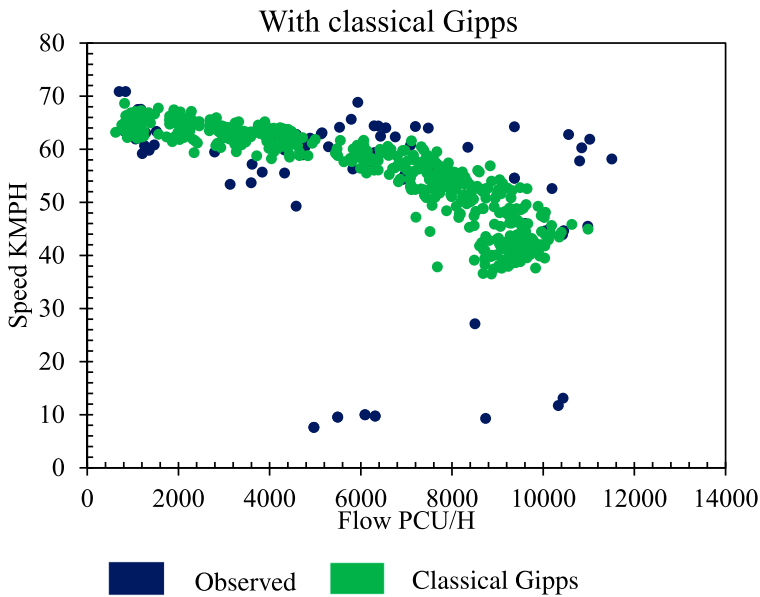
Figure 18. Comparison of speed flow plots: Observed data and classical Gipps model results.

reported in Table 7. The analysis showed that for customized models, the *p*-values range from .71 to .92 for IDM and .71 to .96 for the Gipps model. Whereas, for classical models, the *p*-value is in the range of .32–.75, which signifies a wide range of deviation from the actual field data in the case of classical models. This infers that the customized models perform better in replicating the mixed-traffic flow conditions than their classical versions.

Further, the Wilcoxon rank-sum test (Rey and Neuhäuser 2011; Harris and Hardin 2013) was conducted for each of the vehicle categories between the observed and simulated microscopic data to

Table 7. Probability (p)-values from chi-square test @ 5% level of significance.

Model	Parameter	Motorized three wheelers	Motorized two wheelers	Bus	Car	Truck	LCV
Customized IDM	Relative velocity	0.91	0.75	0.81	0.87	0.71	0.82
	Distance gap	0.87	0.81	0.79	0.92	0.85	0.71
Classical IDM	Relative velocity	0.61	0.52	0.73	0.69	0.45	0.59
	Distance gap	0.76	0.35	0.64	0.75	0.52	0.65
Customized Gipps model	Relative velocity	0.71	0.96	0.75	0.72	0.71	0.93
	Distance gap	0.86	0.75	0.91	0.85	0.89	0.77
Classical Gipps model	Relative velocity	0.54	0.32	0.65	0.52	0.31	0.40
	Distance gap	0.65	0.34	0.60	0.61	0.45	0.49

Table 8. Wilcoxon test statistic over the models with respect to vehicle category.

Model	Parameter	Motorized three wheelers	Motorized two wheelers	Bus	Car	Truck	LCV	Remarks
Customized IDM	Relative velocity	21	18	32	41	46	35	No mean difference exists
	Distance gap	32	41	18	36	51	39	for all vehicle-categories
Classical IDM	Relative velocity	17	12	16	25	11	14	Mean difference exists
	Distance gap	15	17	21	18	32	15	for dominant vehicle-categories
Customized Gipps model	Relative velocity	22	19	35	37	42	33	No mean difference exists
	Distance gap	27	35	16	42	35	21	for all vehicle-categories
Classical Gipps model	Relative velocity	17	10	20	17	10	12	Mean difference exists
	Distance gap	15	19	13	15	25	16	for dominant vehicle-categories

Table 9. Comparison of macroscopic traffic characteristics.

Following Model	Free speeds (kmph)	Optimum speed (kmph)	Capacity (PCU/h/direction)	Deviation from observed capacity value (%)
Observed data	62–70	50	11,960	–
Customized IDM	66	48	12,010	0.4
Classical IDM	60–65	35	13,500	12.8
Customized Gipps	60–70	46	11,900	−0.5
Classical Gipps	62–70	40	10,900	−8.8

test hypotheses the significant difference. The Wilcoxon table's critical value is found to be '16' at a 5 percent level of significance. To accept the null hypothesis: no variation was found in the data. The test statistic values should not be less than critical value 16, and test statistic values are reported in Table 8. From the comparison, it is identified that the customized model output test statistic value is greater than or equal to 16, which advocates no variation in data.

To compare the macroscopic characteristics, boundary conditions such as free speeds, optimum speed and capacity values are compared as reported in Table 9.

From the comparison, as illustrated in Table 9, it is inferred that customized models replicate the mixed-traffic flow characteristics better than their classical versions at both microscopic and macroscopic levels and hold much promise in developing a new framework for modeling mixed-traffic flow conditions. Moreover, Classical IDM overestimates capacity value by about 12.8%, whereas the classical-Gipps model underestimates capacity value by about 8.8%.

The study established that unlike under homogeneous traffic conditions, lateral behavior (lane changing as a traffic state function) is generally discretized in nature. However, under mixed-traffic conditions due to the presence of different vehicle categories and weak lane discipline, both longitudinal and lateral movements are discretely continuous and captured simultaneously based on the presence of surrounding vehicles. It is witnessed that, by applying established following behavior

models developed based on homogeneous-traffic-conditions logic will result in inaccurate outcomes, and hence by customizing them with lateral behavior logic, their performances can be improved.

From the v/V, S_{min}/S and L/L_c factors over different vehicle categories under mixed-traffic stream, it was observed that mainly smaller vehicle categories, such as motorized three-wheelers and Motorized two-wheelers tends to have some extra lateral freedom in the traffic stream as compared to other vehicle categories. As a result, v/V distributions of these vehicle categories are found to be substantially varied from other vehicle categories, similarly L/L_c values are in the range of 0–1.2 for motorized three-wheelers and Motorized two-wheelers in comparison for other vehicles are in the range of 0–0.5. This signifies the amount of lateral freedom available for these vehicles. Finally, it is inferred that mainly smaller vehicles in the traffic stream, by their size and better maneuverability, play a major role in inducing the mixed traffic conditions. Given the stochastic nature of traffic under non-lane based mixed-traffic conditions, it may be inferred that simulation modeling can be a productive approach. The approach can be used very well, provided simulation model is well-calibrated based on quality traffic flow data, as demonstrated in this case using good quality vehicular trajectory data.

Based on the customized-IDM analysis, it was observed that v/V, S_{min}/S and L/L_c tend to govern the subject vehicle instincts, due to its single regime formulation, less variation was observed in mimicking the mixed-traffic conditions at macroscopic level. Whereas with its classical formulation, customized IDM tend to be linear in nature. These observations strongly support the idea backing IDM for coding autonomous vehicle behavior. On the other hand, in microscopic traffic sense, It was identified that at higher distance gaps, the velocity of the subject vehicle is governed by only v/V mainly with negligible values of S_{min}/S and L/L_c, as a result the vehicle will be in acceleration phase to attain its desired velocity, due to which the data was skewed towards the right side axis. Whereas, at less distance gaps S_{min}/S and L/L_c will come in to picture and govern the vehicle instincts and resulted hysteresis phenomenon among the vehicles and tends to match with field hysteresis. On the other hand, in case of micro-level hysteresis, it was observed that based on L/L_c factors the customized IDM is able to mimic the field hysteresis phenomenon well, whereas with its classical formulation, the plots are slender in nature, due to the ascendency of S_{min}/S in the model.

In the case of customized-Gipps model, it is witnessed that due to its multi-regime formulation, at a macroscopic level, the model can replicate the variation in observed speed–flow plots better than customized-IDM results. Simultaneously, while comparing for microscopic hysteresis phenomenon with classical-Gipps formulation, its multi-regime nature is observed. As a result of multi-regime logic, there is a sudden change in the shape of the hysteresis plots, particularly slenderness nature is reflected, when the vehicular pairs are nearing the safety time gap. Whereas, adopting to customized-Gipps model, this nature is well incorporated by inducing a parameter ratio L/L_c in the model. The ratio governs the whole process with lateral behavior instead of directly accepting the safety time gap with its leader vehicles. Due to this logic implemented in the customized-Gipps model, the subject vehicles are switching laterally as a function of L/L_c ratio. Due to this logic, customized-Gipps model can capture variations in relative velocities and distance well, even at lower distance gaps.

Conclusions

The study shows that driving behavior under mixed-traffic environment is unique nature, as it involves simultaneous vehicular movements from different vehicle categories in longitudinal and lateral directions. Nevertheless, frameworks related to appraising the driving behavior under mixed-traffic streams are limited in the body of literature. Interestingly, in this research work, an attempt is made to modify driving behavior logic in selected car-following formulations (IDM and Gipps) and expand them with the dominance of lateral behavior of vehicles in the mixed-traffic stream. Given this research gap, it is well illustrated that the performance of the subject vehicle's lateral behavior depends on surrounding vehicle types and customization of critical parameters such as ratio related to lateral clearance (L/L_c) and binary dummy variable (ω). To check the credibility of customized models microsimulation tool VISSIM 11.0 tool was deployed in the present work. With the help of trajectory data under mixed

traffic conditions, the customized behavior model's performance was investigated at different stages. From research investigations, at the microscopic level, the customized versions can mimic field variation better, and the classical versions fall short in this direction. At the macroscopic level, it is well illustrated that the customized IDM and Gipps models can replicate the observed traffic characteristics more accurately with a deviation of less than 1% in observed capacity values. Whereas, Classical IDM overestimates capacity value by about 12.8%, while classical-Gipps model underestimates capacity value by about 8.8%. Finally, it is quite evident that the models prove their reputation in modeling the mixed traffic conditions also with appropriate induction of lateral-behavior related parameters. Given this, the presented research work can be considered one of the attempts to expand the body of literature and significantly contribute to modeling traffic flow under mixed traffic conditions.

Acknowledgment

Disclosure statement

No potential conflict of interest was reported by the author(s).

ORCID

Narayana Raju http://orcid.org/0000-0002-3561-5676
Shriniwas Arkatkar http://orcid.org/0000-0002-1804-9465
Said Easa http://orcid.org/0000-0003-0754-138X
Gaurang Joshi http://orcid.org/0000-0002-3241-1598

References

Antonov, Peter I., and Vladimir N. Kurlov. 2002. "Evaluation of Ramp Control Algorithms Using Microscopic Traffic Simulation." *Transportation Research Part C: Emerging Technologies* 10 (3): 229–256.

Bärgman, Jonas, Kip Smith, and Julia Werneke. 2015. "Quantifying Drivers' Comfort-zone and Dread-zone Boundaries in Left Turn Across Path/Opposite Direction (LTAP/OD) Scenarios." *Transportation Research Part F: Traffic Psychology and Behaviour* 35: 170–184. doi:10.1016/j.trf.2015.10.003.

Ben-Akiva, Moshe, David Cuneo, Masroor Hasan, Mithilesh Jha, and Qi Yang. 2003. "Evaluation of Freeway Control Using a Microscopic Simulation Laboratory." *Transportation Research Part C: Emerging Technologies* 11 (1): 29–50.

Bharadwaj, Nipjyoti, Pallav Kumar, Shriniwas Arkatkar, Akhilesh Maurya, and Gaurang Joshi. 2016. "Traffic Data Analysis Using Image Processing Technique on Delhi – Gurgaon Expressway." *Current Science* 110 (5). doi:10.18520/cs/v110/i5/808-822.

Boer, Erwin R. 1999. "Car Following from the Driver's Perspective." *Transportation Research Part F: Traffic Psychology and Behaviour* 2 (4): 201–206.

Brackstone, Mark, and Mike McDonald. 1999. "Car-following: A Historical Review." *Transportation Research Part F: Traffic Psychology and Behaviour* 2 (4): 181–196. doi:10.1016/S1369-8478(00)00005-X.

Chen, Danjue, Jorge Laval, Zuduo Zheng, and Soyoung Ahn. 2012. "A Behavioral Car-following Model That Captures Traffic Oscillations." *Transportation Research Part B: Methodological* 46 (6): 744–761.

Chen, Chenyi, Li Li, Jianming Hu, and Chenyao Geng. 2010. "Calibration of MITSIM and IDM Car-following Model Based on NGSIM Trajectory Datasets." Proceedings of 2010 IEEE International Conference on Vehicular Electronics and Safety, ICVES 2010. doi:10.1109/ICVES.2010.5550943.

Chen, Xi-Qun, Wei-Jun Xie, Jing Shi, and Qi-Xin Shi. 2010. "Perturbation and Stability Analysis of the Multi-anticipative Intelligent Driver Model." *International Journal of Modern Physics C* 21 (05): 647–668.

Das, Sanhita, Narayana Raju, Akhilesh Kumar Maurya, and Shriniwas Arkatkar. 2020. "Evaluating Lateral Interactions of Motorized Two-wheelers Using Multi-gene Symbolic Genetic Programming." In *Transportation Research Record*. Los Angeles, CA: Sage Publications. 0361198120934476.

Derbel, Oussama, Tamás Péter, Benjamin Mourllion, and Michel Basset. 2018. "Generalized Velocity–Density Model Based on Microscopic Traffic Simulation." *Transport* 33 (2): 489–501. doi:10.3846/16484142.2017.1292950.

Derbel, Oussama, Tamas Peter, Hossni Zebiri, Benjamin Mourllion, and Michel Basset. 2013. "Modified Intelligent Driver Model for Driver Safety and Traffic Stability Improvement." *IFAC Proceedings Volumes* 46: 744–749. doi:10.3182/20130904-4-JP-2042.00132.

Eggert, Julian, Florian Damerow, and Stefan Klingelschmitt. 2015. The Foresighted Driver Model." IEEE Intelligent Vehicles Symposium (IV), Proceedings, 322–329.

FHWA. 2007. "Next Generation Simulation, FHWA." https://ops.fhwa.dot.gov/trafficanalysistools/ngsim.htm.

Forbes, T. W., M. J. Zagorski, E. L. Holshouser, and W. A. Deterline. 1959. "Measurement of Driver Reaction to Tunnel Conditions." *Proceedings of the Highway Research Board* 35: 345–357.

Gazis, Denos C, Robert Herman, and Renfrey B Potts. 1959. "Car-following Theory of Steady-state Traffic Flow." *Operations Research* 7 (4): 499–505. doi:10.1287/opre.7.4.499.

Gazis, Denos C., Robert Herman, and Richard W. Rothery. 1961. "Nonlinear Follow-the-Leader Models of Traffic Flow." *Operations Research* 9 (4): 545–567.

Gipps, P. G. 1981. "A Behavioural Car-following Model for Computer Simulation." *Transportation Research Part B: Methodological* 15 (2): 105–111. doi:10.1016/0191-2615(81)90037-0.

Gunay, Banihan. 2007. "Car Following Theory with Lateral Discomfort." *Transportation Research Part B: Methodological* 41 (7): 722–735. doi:10.1016/j.trb.2007.02.002.

Gurusinghe, Gemunu Senadeera, Takashi Nakatsuji, Yoichi Azuta, Prakash Ranjitkar, and Yordphol Tanaboriboon. 2002. "Multiple Car-following Data with Real-time Kinematic Global Positioning System." *Transportation Research Record: Journal of the Transportation Research Board* 1802 (1): 166–180. doi:10.3141/1802-19.

Guzman, Luis A., and Juan Pablo Orjuela. 2017. "Linking a Transport Dynamic Model with an Emissions Model to Aid Air Pollution Evaluations of Transport Policies in Latin America." *Transportmetrica B: Transport Dynamics* 5 (3): 265–280.

Harris, Tammy, and James W. Hardin. 2013. "Exact Wilcoxon Signed-rank and Wilcoxon Mann–Whitney Ranksum Tests." *The Stata Journal: Promoting Communications on Statistics and Stata* 13 (2): 337–343.

Hidas, Peter. 2002. "Modelling Lane Changing and Merging in Microscopic Traffic Simulation." *Transportation Research Part C: Emerging Technologies* 10 (5-6): 351–371.

Jie, Li, Henk Van Zuylen, Yusen Chen, Francesco Viti, and Isabel Wilmink. 2013. "Calibration of a Microscopic Simulation Model for Emission Calculation." *Transportation Research Part C: Emerging Technologies* 31: 172–184.

Johansson, Gunnar, and Kåre Rumar. 1971. "Drivers' Brake Reaction Times." *Human Factors: The Journal of the Human Factors and Ergonomics Society* 13 (1): 23–27.

Kanagaraj, Venkatesan, Gowri Asaithambi, Tomer Toledo, and Tzu-Chang Lee. 2015. "Trajectory Data and Flow Characteristics of Mixed Traffic." *Transportation Research Record: Journal of the Transportation Research Board* 2491: 1–11. doi:10.3141/2491-01.

Keyvan-Ekbatani, Mehdi, Victor L. Knoop, and Winnie Daamen. 2016. "Categorization of the Lane Change Decision Process on Freeways." *Transportation Research Part C: Emerging Technologies* 69: 515–526.

Koutsopoulos, Haris N., and Haneen Farah. 2012. "Latent Class Model for Car Following Behavior." *Transportation Research Part B: Methodological* 46 (5): 563–578.

Kumar, Pallav, Narayana Raju, Ayush Mishra, Shriniwas S Arkatkar, and Gaurang Joshi. 2018. "Validating Area Occupancy-based Passenger Car Units and Homogeneous Equivalent Concept Under Mixed Traffic Conditions in India." *Journal of Transportation Engineering, Part A: Systems* 144 (10): 04018064.

Laquai, Florian, Claudio Gusmini, Marcus Tonnis, Gerhard Rigoll, and Gudrun Klinker. 2013. "A Multi Lane Car Following Model for Cooperative ADAS." 16th International IEEE Conference on Intelligent Transportation Systems (ITSC 2013), 1579–1586. IEEE.

Laws, Car-following. 1981. "Characterization of Traffic Oscillation Propagation Under Nonlinear Car-following Laws." *Environmental Engineering* 12 (January 2011): 1–5.

Lee, Won Do, Wim Ectors, Tom Bellemans, Bruno Kochan, Davy Janssens, Geert Wets, Keechoo Choi, and Chang Hyeon Joh. 2018. "Investigating Pedestrian Walkability Using a Multitude of Seoul Data Sources." *Transportmetrica B: Transport Dynamics* 6 (1): 54–73.

Li, Keqiang Wang, Xiao Wang, Youchun Xu, and Jianqiang Wang. 2016. "Lane Changing Intention Recognition Based on Speech Recognition Models." *Transportation Research Part C: Emerging Technologies* 69: 497–514.

Lima Azevedo, Carlos, Biagio Ciuffo, João Lourenço Cardoso, and Moshe E. Ben-Akiva. 2015. "Dealing with Uncertainty in Detailed Calibration of Traffic Simulation Models for Safety Assessment." *Transportation Research Part C: Emerging Technologies* 58: 395–412.

Løvås, Gunnar G. 1994. "Modeling and Simulation of Pedestrian Traffic Flow." *Transportation Research Part B: Methodological* 28 (6): 429–443.

Mallikarjuna, C., and K. R. Rao. 2011. "Heterogeneous Traffic Flow Modelling: A Complete Methodology." *Transportmetrica* 7 (5): 321–345.

Milanés, Vicente, and Steven E. Shladover. 2014. "Modeling Cooperative and Autonomous Adaptive Cruise Control Dynamic Responses Using Experimental Data." *Transportation Research Part C: Emerging Technologies* 48: 285–300.

Newell, G. F. 1961. "Nonlinear Effects in the Dynamics of Car Following." *Operations Research* 9 (2): 209–229.

Ngoduy, D. 2012. "Application of Gas-kinetic Theory to Modelling Mixed Traffic of Manual and ACC Vehicles." *Transportmetrica* 8 (1): 43–60.

Okuda, Hiroyuki, Nobuto Sugie, and Tatsuya Suzuki. 2018. "Real-time Collision Avoidance Control Based on Continuation Method for Nonlinear Model Predictive Control with Safety Constraint." Asian Control Conference, ASCC 2017, 1086–1091. doi:10.1109/ASCC.2017.8287322.

Oviedo-Trespalacios, Oscar, Md Mazharul Haque, Mark King, and Simon Washington. 2017. "Effects of Road Infrastructure and Traffic Complexity in Speed Adaptation Behaviour of Distracted Drivers." *Accident Analysis and Prevention* 101: 67–77.

Papathanasopoulou, Vasileia, and Constantinos Antoniou. 2015. "Towards Data-driven Car-following Models." *Transportation Research Part C: Emerging Technologies* 55: 496–509. doi:10.1016/j.trc.2015.02.016.

Patil, Shubham, Narayana Raju, Shriniwas Arkatkar, and Said Easa. 2021. *Modeling Vehicle Collision Instincts Over Road Midblock Using Deep Learning.*

Paul, Geetashree, Narayana Raju, Shriniwas Arkatkar, and Said Easa. 2021. "Can Segregating Vehicles in Mixed-traffic Stream Improve Safety and Throughput? Implications Using Simulation." *Transportmetrica A: Transport Science* 17 (4): 1002–1026.

Pipes, Louis A. 1953. "An Operational Analysis of Traffic Dynamics." *Journal of Applied Physics* 24 (3): 274–281. doi:10.1063/1.1721265.

Pourabdollah, Mitra, Eric Bjarkvik, Florian Furer, Bjorn Lindenberg, and Klaas Burgdorf. 2017. "Calibration and Evaluation of Car Following Models Using Real-world Driving Data." IEEE 20th International Conference on Intelligent Transportation Systems (ITSC), 1–6. IEEE.

Rahmati, Yalda, Mohammadreza Khajeh Hosseini, Alireza Talebpour, Benjamin Swain, and Christopher Nelson. 2019. "Influence of Autonomous Vehicles on Car-following Behavior of Human Drivers." *Transportation Research Record: Journal of the Transportation Research Board* 2673 (12): 367–379.

Raju, Narayana, Shriniwas Arkatkar, and Joshi Gaurang. 2019. "Replicating Driving Behavior Under Heterogeneous Non-lane-based Traffic Environment: A Supervised Machine Learning Based Methodology." *Journal of the Eastern Asia Society for Transportation Studies* 13: 1801–1816. https://www.jstage.jst.go.jp/article/easts/13/0/13_1801/_article/-char/ja/.

Raju, Narayana, Shriniwas Arkatkar, and Gaurang Joshi. 2020. "Evaluating Performance of Selected Vehicle Following Models Using Trajectory Data Under Mixed Traffic Conditions." *Journal of Intelligent Transportation Systems* 24: 617–634.

Raju, Narayana, Pallav Kumar, Aayush Jain, Shriniwas S. Arkatkar, and Gaurang Joshi. 2018. "Application of Trajectory Data for Investigating Vehicle Behavior in Mixed Traffic Environment." *Transportation Research Record: Journal of the Transportation Research Board* 2672 (43): 122–133.

Raju, Narayana, Pallav Kumar, Chakradhar Reddy, Shriniwas Arkatkar, and Gaurang Joshi. 2017. "Examining Smoothening Techniques for Developing Vehicular Trajectory Data Under Heterogeneous Conditions." *Journal of the Eastern Asia Society for Transportation Studies* 12: 1549–1568. Eastern Asia Society for Transportation Studies.

Rakha, Hesham, and Brent Crowther. 2002. "Comparison of Greenshields, Pipes, and Van Aerde Car-following and Traffic Stream Models." *Transportation Research Record: Journal of the Transportation Research Board* 1802 (1): 248–262. doi:10.3141/1802-28.

Rakha, Hesham, and Weidong Wang. 2009. "Procedure for Calibrating Gipps Car-following Model." *Transportation Research Record: Journal of the Transportation Research Board* 2124: 113–124. doi:10.3141/2124-11.

Ranjitkar, Prakash, Takashi Nakatsuji, and Akira Kawamua. 2005. "Car-following Models: An Experiment Based Benchmarking." *Journal of the Eastern Asia Society for Transportation Studies* 6: 1582–1596.

Rey, Denise, and Markus Neuhäuser. 2011. "Wilcoxon-signed-rank Test." *International Encyclopedia of Statistical Science*, 1658–1659. doi:10.1007/978-3-642-04898-2_616.

Savolainen, Peter, Timothy Gates, Ryan Todd, Tapan Datta, and Jill G. Morena. 2012. "Lateral Placement of Motor Vehicles When Passing Bicyclists." *Transportation Research Record: Journal of the Transportation Research Board* 2314 (2314): 14–21. doi:10.3141/2314-03.

Sharath, M. N., and Nagendra R. Velaga. 2020. "Enhanced Intelligent Driver Model for Two-dimensional Motion Planning in Mixed Traffic." *Transportation Research Part C: Emerging Technologies* 120: 102780.

Tang, Tie Qiao, Jian Zhang, Liang Chen, and Hua Yan Shang. 2017. "Analysis of Vehicle's Safety Envelope Under Car-following Model." *Physica A: Statistical Mechanics and Its Applications* 474: 127–133. doi:10.1016/j.physa.2017.01.076.

Toledo, Tomer, Haris N. Koutsopoulos, and Moshe Ben-Akiva. 2003. "Modeling Integrated Lane-changing Behavior." *Transportation Research Record: Journal of the Transportation Research Board* 1857 (1): 30–38. doi:10.3141/1857-04.

Toledo, Tomer, Haris N. Koutsopoulos, and Moshe Ben-Akiva. 2009. "Estimation of an Integrated Driving Behavior Model." *Transportation Research Part C: Emerging Technologies* 17 (4): 365–380.

Treiber, Martin, Ansgar Hennecke, and Dirk Helbing. 2000. "Congested Traffic States in Empirical Observations and Microscopic Simulations." *Physical Review E* 62 (2): 1805–1824.

van Winsum, Wim. 1999. "The Human Element in Car Following Models." *Transportation Research Part F: Traffic Psychology and Behaviour* 2 (4): 207–211. doi:10.1016/S1369-8478(00)00008-5.

Venkatesan, Kanagaraj, A. Gowri, and R. Sivanandan. 2008. "Development of Microscopic Simulation Model for Heterogeneous Traffic Using Object Oriented Approach." *Transportmetrica* 4 (3): 227–247.

Venthuruthiyil, Suvin P., and Mallikarjuna Chunchu. 2018. "Trajectory Reconstruction Using Locally Weighted Regression: A New Methodology to Identify the Optimum Window Size and Polynomial Order." *Transportmetrica A: Transport Science* 14 (10): 881–900.

Vicraman, Vivek, Caleb Ronald, Tom Mathew, and K. V. Rao. 2014. *Traffic Data Extractor.* Bombai: IIT. http://www.civil.iitb.ac.in/tvm/tde2.

VISSIM. P T V Vision. "Ptv Vissim Drivermodel Dll Interface Documentation.".

Wang, Xin, Asad J. Khattak, Jun Liu, Golnush Masghati-Amoli, and Sanghoon Son. 2015. "What Is the Level of Volatility in Instantaneous Driving Decisions?" *Transportation Research Part C: Emerging Technologies* 58: 413–427.

Wiedemann, Rainer. 1974. *Simulation Des Straßenverkehrsflusses. Schriftenreihe Des IfV, 8, Institut Für Verkehrswesen*. Karlsruhe: Universität Karlsruhe.

Xu, Xinyue, Haiying Li, Jun Liu, Bin Ran, and Lingqiao Qin. 2019. "Passenger Flow Control with Multi-station Coordination in Subway Networks: Algorithm Development and Real-world Case Study." *Transportmetrica B: Transport Dynamics* 7 (1): 446–472.

Yang, D., Y. Pu, L.-L. Zhu, F. Yang, and R. Bin. 2013. "Improved Safe Distance Car-following Model." *Beijing Gongye Daxue Xuebao/Journal of Beijing University of Technology* 39 (9): 1335–1342.

Yang, Da, Liling Zhu, Yalong Liu, Danhong Wu, and Bin Ran. 2018. "A Novel Car-following Control Model Combining Machine Learning and Kinematics Models for Automated Vehicles." *IEEE Transactions on Intelligent Transportation Systems* 20 (6): 1991–2000.

Yeung, Jian Sheng, and Yiik Diew Wong. 2014. "The Effect of Road Tunnel Environment on Car Following Behaviour." *Accident Analysis and Prevention* 70: 100–109.

Zhang, Xiaohui, Jie Sun, Xiao Qi, and Jian Sun. 2019. "Simultaneous Modeling of Car-following and Lane-changing Behaviors Using Deep Learning." *Transportation Research Part C: Emerging Technologies* 104: 287–304.

Zheng, Zuduo. 2014. "Recent Developments and Research Needs in Modeling Lane Changing." *Transportation Research Part B: Methodological* 60: 16–32.

Zhu, Feng, Hong K. Lo, and Hong Zhi Lin. 2013. "Delay and Emissions Modelling for Signalised Intersections." *Transportmetrica B: Transport Dynamics* 1 (2): 111–135.

Appendix

Coded driving behavior in simulation models along with YouTube videos

Trial 1: Initial trials for coding driving behavior: In the present trial, some vehicle abruptly stops over the road space due to bugs in code. https://www.youtube.com/watch?v = ZKCsT0TuKx8

Trial 2: In this trial, due to some angular glitz in coding driving behavior, vehicles are randomly moving over the road section. https://www.youtube.com/watch?v = KqF1×2zAX7c

Trial 3: In this trial, only the following behavior of vehicles is coded with on passing of vehicles. As a result, only vehicles are following each other without any overtaking/passing. https://www.youtube.com/watch?v = ouTCEFqhOPM

Trial 4: In this trial, the conceptualized logic of driving behavior explained the paper was coded in simulation. Due to some random glitz, few vehicles are assigning a high magnitude of a longitudinal angle. https://www.youtube.com/watch?v = YU5UoZ5h6NQ

Final code version: This is the final version of coded driving behavior with conceptualized logic, as a part of research work IDM and Gipp's models were assigned for modeling driving behavior. Volume 1: https://www.youtube.com/watch?v = v5xPTHl3oRQ

Volume 2: https://www.youtube.com/watch?v = tm_0FKlK19E